

## Results

### Identification of the genes required in the miRNA pathway by random gene disruption

To identify genes involved in miRNA pathways especially in liver cells, we constructed a reporter carrying a hygromycin resistance gene with two miR122-responsive elements in its 3'-UTR (Fig. 1A). We chose miR122 because it is the most abundant and tissue-specific miRNA in the liver [16]. Binding of miR122 reduces the expression of this hygromycin resistance gene in this construct. However, if miR122 function is impaired by the disruption of genes that are important for miRNA signaling, hygromycin resistance gene expression increases. Cells carrying such disrupted genes will therefore survive hygromycin treatment. Additionally, to enhance the effects of miR122, we co-transfected a miR122 precursor-expressing plasmid (Fig. 1A) with the reporter construct and selected monoclonal cells containing both constructs to minimize the effects of their random integration. After infection with retroviruses carrying a blasticidin resistance gene to produce random gene disruption in the selected reporter cells, cells surviving hygromycin treatment were harvested. The disrupted genes in the surviving cells were identified by 3' RACE. We infected  $\sim 10^6$  Huh7-pBS-Hygro-miR122 cells established from Huh7 cells and obtained  $\sim 10^4$  clones with random gene disruptions (confirmed by resistance to blasticidin) (Fig. 1B). After hygromycin selection, ten clones in which miRNA function was apparently impaired were obtained. In these ten clones, six disrupted genes were successfully identified (Table 1). One of them, RACK1 (also known as GNB2L1), appeared in duplicate and was found to be disrupted in two clones.

### Requirement of RACK1 for microRNA function

Of the genes identified, RACK1 was found to be disrupted in two independent clones (Table 1). RACK1 was previously identified as the binding partner of eIF6, a ribosome inhibitory protein known to prevent proper assembly of the 80S ribosome, and contributes to miRNA silencing by associating with RISC [17–19]. However, the requirement for eIF6 in miRNA function is controversial because other models, in which miRNA silencing is mediated by Ago2 (eIF2C2) and an interaction with eIF4E [20], or by GW182 [21], have more recently been described.

To confirm the requirement for RACK1 in miRNA function, we measured miRNA activity using a reporter assay involving transient expression of an siRACK1 construct and an miRNA precursor-overexpression plasmid. Transient knockdown of RACK1 reduced the function of three miRNAs: miR122, miR140, and miR185 (Fig. 2A). To examine these effects using a natural 3'-UTR containing miR122 binding sites, we used a CatA-Luc reporter that carried the 3'-UTR of the CAT1 (cationic amino acid transporter 1) gene and a luciferase gene [22]. The CAT1 3'-UTR contains three predicted miR122 binding sites [22]. The requirement for RACK1 in miRNA function was confirmed using this reporter construct (Fig. 2B).

Next, we established stable RACK1-knockdown Huh7 cells (Fig. 2C) and compared the effects of miRNAs in control and RACK1-knockdown cells. Consistent with the results of the transient transfection assays, RACK1-knockdown cells showed weaker miRNA mediated-inhibition of target gene expression in a reporter system involving miR185 precursor-expressing plasmids and its reporter constructs (Fig. 2D). To measure changes in endogenous miRNA function in RACK1-knockdown cells, control and RACK1-knockdown cells were transfected with reporter constructs specific for several miRNAs and luciferase activity was then measured. We confirmed the inhibition of endogenous miRNA function in RACK1-knockdown cells (Fig. 2E). These

results suggest that RACK1 is indeed required for miRNA function.

### RACK1 may function after miRNA maturation but before the expression-inhibitory machinery

To identify the point at which RACK1 enhances miRNA function, mature miRNA levels were first measured in stable RACK1-knockdown cells. Levels of endogenous mature miR122, miR22, miR140-5p, -3p, and miR185, which are expressed at relatively high levels in liver cells [16], were comparable in control and RACK1-knockdown cells (Fig. 3A and Figure S1). This suggests that RACK1 may not be involved in miRNA maturation. We next showed that overexpression of artificial synthetic miRNA oligonucleotides replicated normal miRNA-mediated inhibition of gene expression in RACK1-knockdown cells (Fig. 3B). These results suggest that, *in vivo*, RACK1 may function after miRNA maturation, but before the expression-inhibiting machinery in the natural miRNA pathway, although the finding that the synthetic mature miRNAs were functional even in Ago2-knockdown cells (Figure S2A, B) indicates that their function might be Ago2-independent. Additionally, the expression of Droscha, DGCR8, Dicer, TRBP, Ago1, Ago2, Ago3, Ago4, and eIF4E, all of which are known to be involved in the miRNA pathway, were almost similar in control and RACK1-knockdown cells (Fig. 3C). Furthermore, the localization and number of the p-bodies, which may be involved in miRNA-mediated silencing [23,24], were not markedly affected by RACK1-knockdown (as determined by staining for the intracellular marker GW182) [23] (Fig. 3D). These results suggest that RACK1 functions after miRNA maturation, but before mature miRNAs exert their expression-inhibitory effects.

### RACK1 interacts with KSRP and is required for the full recruitment of mature miRNAs to the RISC

To determine whether RACK1 interacts with miRNA pathway related-molecules, transiently-transfected myc-tagged RACK1 was first immunoprecipitated. While myc-tagged RACK1 was efficiently precipitated (Fig. 4A), RISC constituent proteins such as Dicer, DDX20 (Gemin3) and Gemin4 [25] were found not to interact with RACK1 (Fig. 4A). GW182 did not interact with RACK1 (Fig. 4A). eIF6, which was previously reported to interact with RACK1 [18] and which may be involved in miRNA silencing [19], did not show an interaction with RACK1 in the present study (Fig. 4A). However, Ago2 weakly interacted with RACK1 (Fig. 4A), as reported recently [26]. Moreover, KH-type splicing regulatory protein (KSRP; also known as KHSRP), a key mediator of mRNA degradation [27,28] and a component of the Dicer complex that promotes the maturation of a subset of miRNAs [29], interacted with RACK1, especially when Dicer was overexpressed (Fig. 4A and Figure S3). This interaction was also confirmed by immunoprecipitation of endogenous RACK1 (Fig. 4B). The interactions of RACK1 with Ago2 and KSRP were insensitive to RNase A treatment (Figure S4), suggesting that they were not mediated by RNAs. Next, because it seemed that RACK1 functioned after miRNA maturation and before mature miRNA recruitment into the RISC, we measured levels of miRNAs in complexes immunoprecipitated using an anti-Ago2 antibody. Levels of mature miRNAs examined in the Ago2-containing complexes were lower in RACK1-knockdown cells than in control cells (Fig. 4C and Figure S5). To determine the possible causes of impaired mature miRNA loading into Ago2-related complexes in RACK1-knockdown cells, we determined the intracellular localization of KSRP and Ago2 in RACK1 knockdown cells (Fig. 4D). While KSRP is distributed both in the nucleus and cytoplasm and Ago2 localizes mainly in

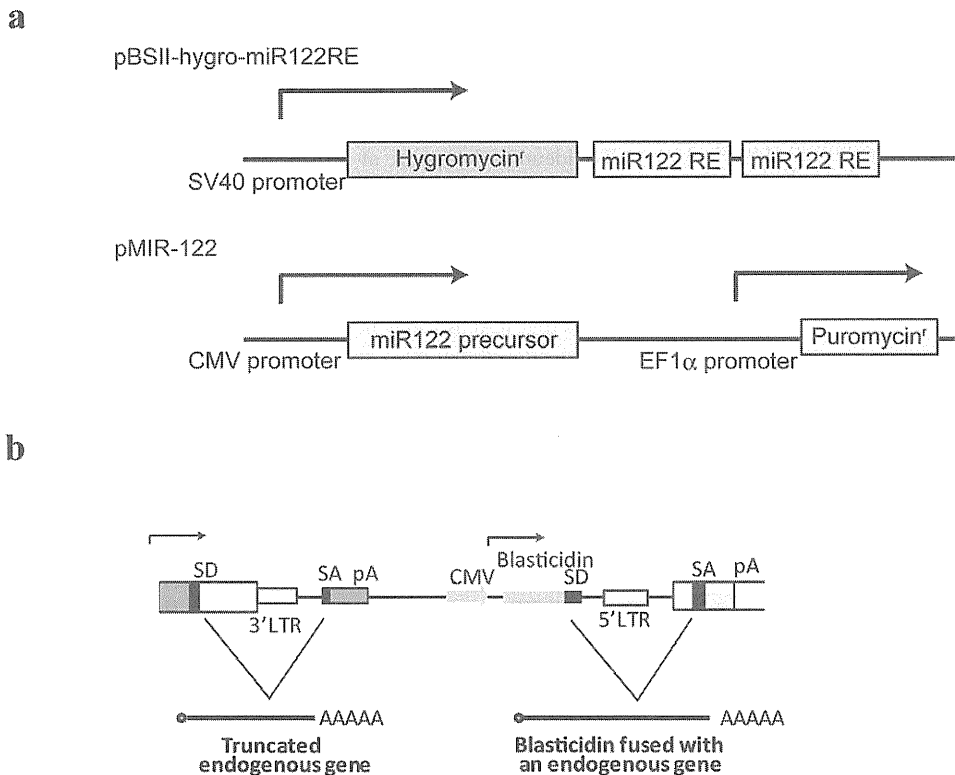


**Figure 1. Constructs used in the study.** **A**, Reporter and miR122 precursor-expressing constructs. A construct containing an SV40 promoter-driven hygromycin resistance gene with two tandem miR122-responsive elements (miR122 RE) in its 3'-UTR was used to assess miRNA function. To express miR122, a construct carrying a CMV promoter-driven miR122 precursor was used in conjunction with puromycin selection. **B**, pDisrupt vector structure and gene products resulting from viral integration. Splicing occurs between the SD (splicing donor) and SA (splicing acceptor) sites (i.e., between the 3'-end of the endogenous gene exon and the retroviral SA site, as well as between the retroviral SD at the 3'-end of the blastidicin gene and the endogenous SA site at the 5'-end of the downstream gene exon). pA, polyadenylation signal. doi:10.1371/journal.pone.0024359.g001

cytoplasm in control cells, KSRP localizes more in the nucleus in RACK1-knockdown cells (Fig. 4D). The changes in the subcellular localization of KSRP in RACK1-knockdown cells were also confirmed by Western blotting using cell lysates prepared after subcellular fractionation (Fig. 4E). The function of synthetic mature miRNAs was not affected by KSRP knockdown (Figure S6A, B), suggesting that KSRP itself is not required for RISC activity. Thus, these localization changes with RACK-1 may be related to the impaired mature miRNA loading into Ago2 complexes from the KSRP-associated complexes, although, because the binding of KSRP

to Ago2 could not be detected in our coimmunoprecipitation study (Figure S7), the precise mechanisms remain to be elucidated. Nonetheless, these results suggest that RACK1 interacts with KSRP and that the recruitment of mature miRNAs into the RISC is impaired in RACK1-knockdown cells.

**RACK1 expression is frequently decreased in liver cancers**

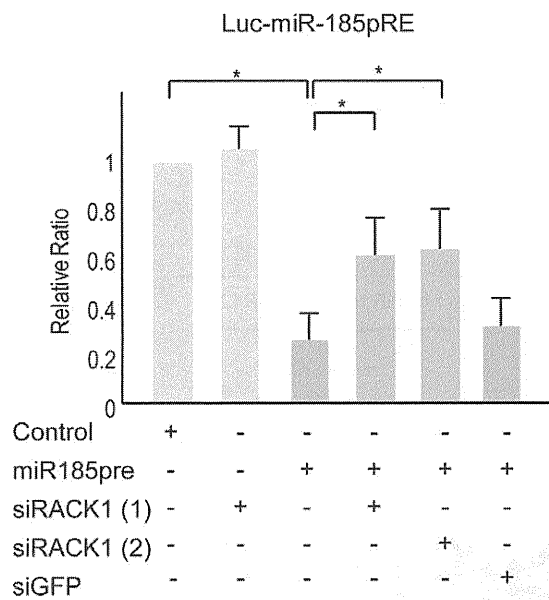
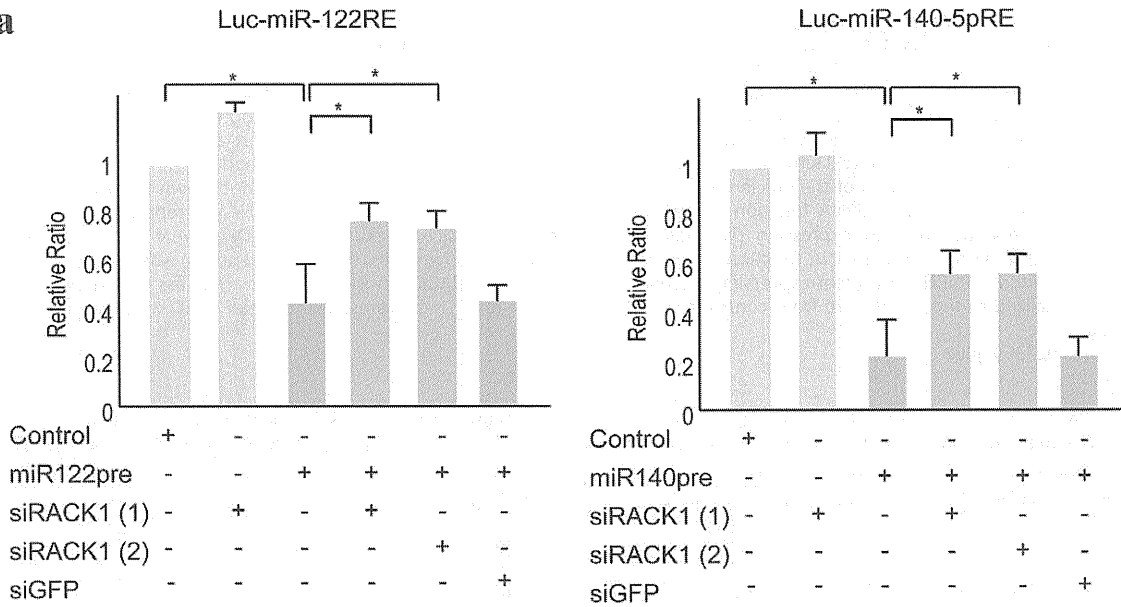
Recent results linking reduced global expression of miRNAs and reduced miRNA function with tumorigenesis [12,30] encouraged us to examine RACK1 expression in cancers. To this end, we

**Table 1.** List of genes identified in this screening.

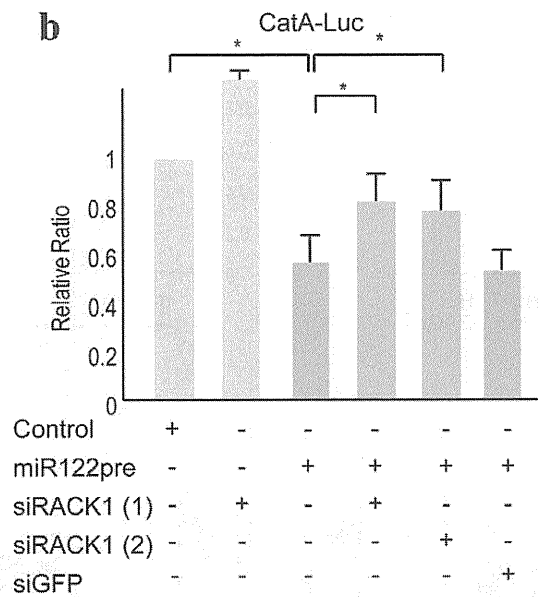
Gene ID	Gene symbol	Gene title	Known function	Also known as
100288263	LOC100288263	hypothetical protein	Unknown	
10399	GNB2L1	guanine nucleotide binding protein (G protein), beta polypeptide 2-like 1	Translation	RACK1, PIG21
10055	SAE1	SUMO1 activating enzyme subunit 1	Sumoylation	AOS1, SUA1, UBLE1A
10399	GNB2L1	guanine nucleotide binding protein (G protein), beta polypeptide 2-like 1	Translation	RACK1, PIG21
6228	RPS23	ribosomal protein S23	Ribosome 40S	FLJ35016
6135	RPL11	ribosomal protein L11	Ribosome 60S	DBA7, GIG34
5358	PLS3	plastin 3	Actin binding	T-plastin

doi:10.1371/journal.pone.0024359.t001

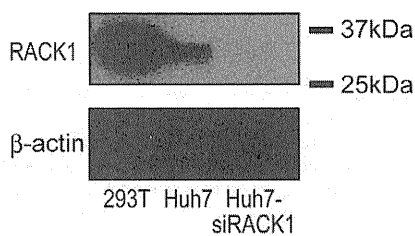
**a**



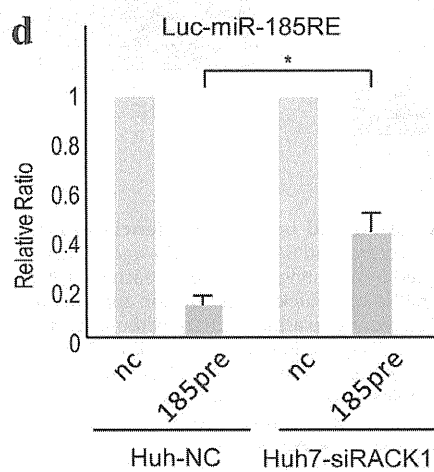
**b**



**c**



**d**



**e**

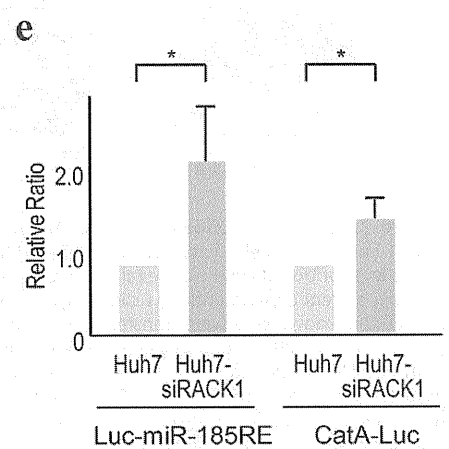


**Figure 2. RACK1 is required for miRNA function.** **A**, Overexpression of miR122, miR140, and miR185 precursors suppressed activity of the corresponding reporters. RACK1 knockdown partially blocked these effects. miRNA reporter plasmids were transfected, with or without the corresponding miRNA precursor- and two types of siRACK1-expressing plasmids (siRACK1 (1) and (2)), into Huh7 cells. Values were normalized to those obtained from cells transfected with a miRNA precursor-non-expressing control vector, which were set to 1. Data represent the mean  $\pm$  SD of three independent experiments. siGFP was used as a control, and it had no effect. Similar results were obtained using PLC/PRF/5 cells. **B**, CatA-Luc plasmids, which contain endogenous miR122 target sites derived from the CAT1 gene in its 3'-UTR, were transfected, with or without miR122 precursor- and siRACK1-expressing plasmids, into Huh7 cells. Data were generated and are presented as described in (A). Similar results were obtained using PLC/PRF/5 cells. **C**, Confirmation of the efficient knockdown of RACK1 expression in stable RACK1-knockdown Huh7 cells. 293T cell lysates were used as a positive control. **D**, miRNA function is impaired in stable RACK1-knockdown cells. miRNA185 reporter plasmids were transfected, with or without miR185 precursor-expressing plasmids, into control and RACK1-knockdown cells. Data were generated and are presented as described in (A). **E**, Endogenous miRNA function is impaired in RACK1-knockdown cells. miRNA185 reporter plasmids and CatA-Luc plasmids were transfected without miRNA precursor-expressing plasmids into control and RACK1-knockdown cells to assess endogenous miRNA function. Values were normalized to those obtained from control cells, which were set to 1. Data represent the mean  $\pm$  SD of three independent experiments. \*,  $p < 0.05$ . doi:10.1371/journal.pone.0024359.g002

determined RACK1 expression in various cancers and in healthy tissues by immunohistochemistry. While RACK1 expression was essentially normal in most cancers, it was frequently reduced in hepatocellular carcinoma (HCC) (Fig. 5A, B, C), consistent with a

previous report [31]. KSRP expression levels were relatively higher in liver tissues than in other organs, but no remarkable expression differences between HCC and adjacent tissues were observed (Figure S8A, B). These results suggest that decreased

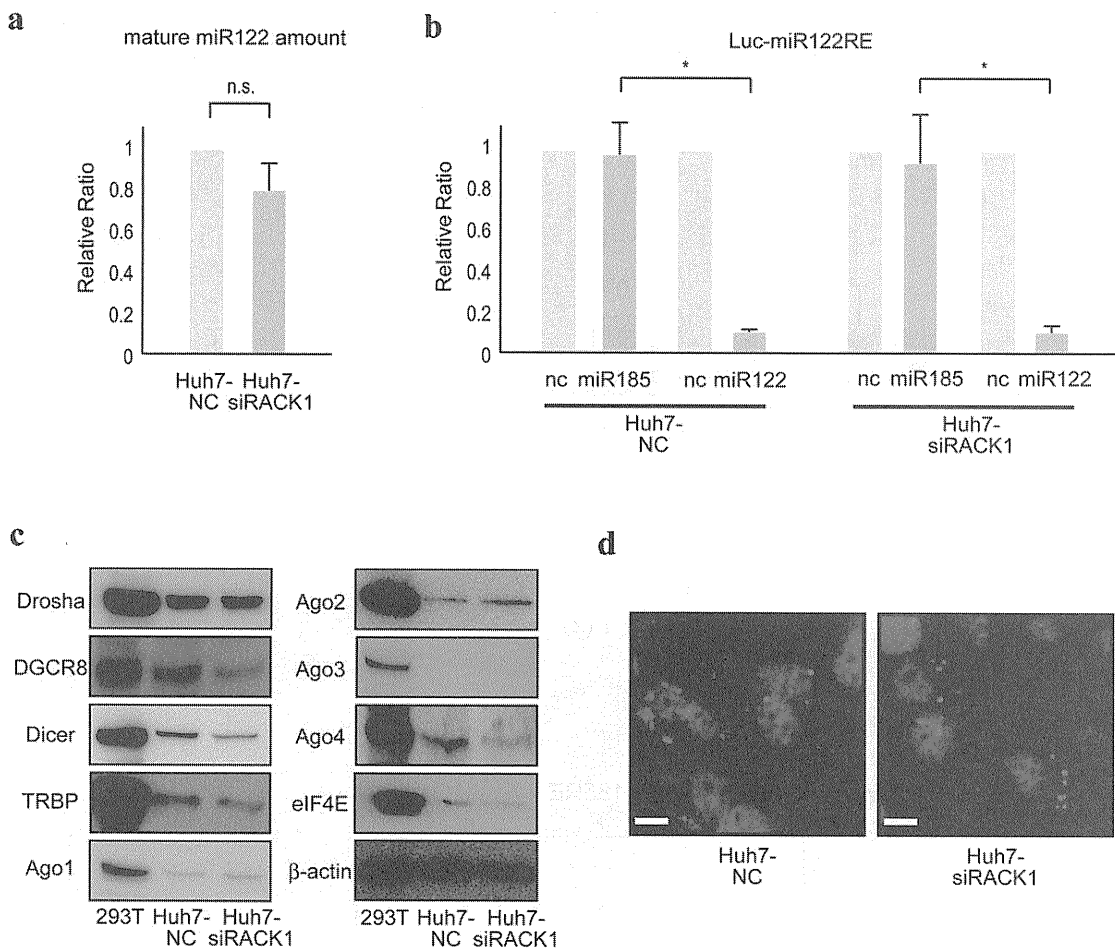


**Figure 3. RACK1 functions after miRNA maturation and before the silencing machinery.** **A**, miRNA maturation was not impaired in RACK1-knockdown cells. Total RNA was isolated from control and RACK1-knockdown cells. Levels of mature miR122 were measured and normalized to the level of U6 snRNA. Relative ratios were calculated by adjusting the value for each miRNA in control cells to 1. Data represent the mean  $\pm$  SD of six independent experiments. **B**, Artificial synthetic miRNA oligonucleotides function appropriately in RACK1-knockdown cells. Control Huh7 cells and RACK1-knockdown cells were transfected with miR122 reporter plasmids with or without synthetic corresponding miR122 oligonucleotides and non-corresponding miR185 oligonucleotides (to verify specificity). Values were normalized to those obtained from the cells transfected with control synthetic oligonucleotides, which were set to 1. Data represent the mean  $\pm$  SD of three independent experiments. \*,  $p < 0.05$ . Similar results were obtained using PLC/PRF/5 cells. **C**, Expression of proteins involved in the miRNA pathway was normal in RACK1-knockdown cells. 293T cell lysates were used as a positive control. **D**, Localization and expression of P-bodies were normal in RACK1-knockdown cells. Control and RACK1-knockdown cells were immunostained for the p-body marker GW182. Scale bar, 50  $\mu$ m. doi:10.1371/journal.pone.0024359.g003

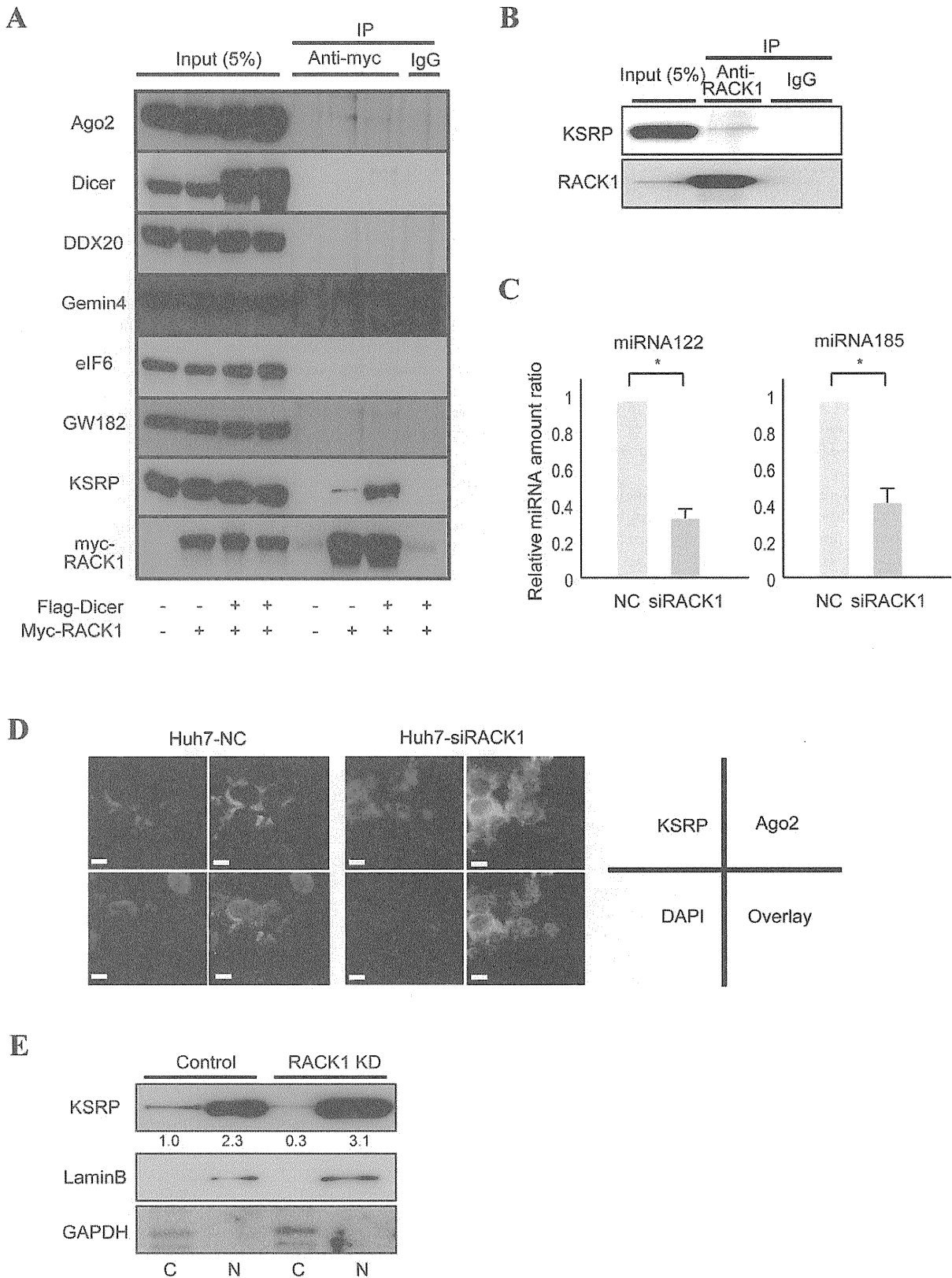


**Figure 4. RACK1 binds to KSRP and may be involved in the recruitment of mature miRNAs to the RISC.** **A**, Huh7 cells were transiently transfected with a control vector or a myc-tagged RACK1-expressing plasmid with or without a flag-tagged Dicer-expressing plasmid. Myc-tagged RACK1 was immunoprecipitated using anti-myc agarose. Normal mouse IgG was used as a control for immunoprecipitation. Co-precipitated proteins were blotted using antibodies against the indicated proteins. Five percent of the total cell lysates was loaded as “input.” Representative results from two independent experiments are shown. Similar results were obtained using 293T cells. **B**, Endogenous RACK1 in Huh7 cells was immunoprecipitated using anti-RACK1 antibody and Protein A/G Sepharose. Normal mouse IgG was used as a control for immunoprecipitation.

Coprecipitated proteins were blotted using antibodies against the indicated proteins. Five percent of the total cell lysate was loaded as “input.” Representative results from two independent experiments are shown. **C**, Levels of mature miR122 and miR185 in Ago2-containing complexes were reduced in RACK1-knockdown cells. Mature miRNA levels were measured in RNA samples isolated from Ago2-containing complexes from control Huh7 (NC) cells and RACK1-knockdown (siRACK1) cells. miRNA levels were calculated as relative ratios. Data represent the mean  $\pm$  SD of six independent experiments. \*,  $p < 0.05$ . **D**, More KSRP localizes in the nucleus in RACK1-knockdown cells. Intracellular localization of KSRP (red) and Ago2 (green) were examined in control and RACK1-knockdown cells. KSRP was distributed both in the nucleus and cytoplasm, but more KSRP localized in RACK1-knockdown cells. Scale bar, 50  $\mu$ m. **E**, Greater localization of KSRP to the nucleus in RACK1-knockdown (RACK1 KD) cells was confirmed by Western blotting. Cytoplasmic (C) and nuclear (N) fractions were blotted with anti-KSRP antibody. The numbers below the panel indicate relative KSRP protein levels. GAPDH (a cytoplasm marker) and Lamin B (a nucleus marker) were blotted to confirm the appropriate fractionation.

doi:10.1371/journal.pone.0024359.g004

RACK1 expression and, consequently, decreased miRNA function may play an important role in HCC.

## Discussion

Here, we have shown that RACK1 is required for miRNA function through comprehensive gene screening using a random gene disruption method. Our results show that RACK1 interacts with KSRP and plays an important role in recruiting mature miRNAs to the RISC. Additionally, the expression of RACK1 is frequently decreased in HCC and may play a role in its pathogenesis.

RACK1 was initially identified as a major component of active ribosomes [18]. It binds directly to eIF6, which keeps the 40S and 60S ribosomal subunits apart, preventing the formation of a translationally competent complex. RACK1 bridges PKC and eIF6. Subsequent phosphorylation of eIF6 by PKC causes eIF6 to be released, an event that triggers 60S subunit activation. More recently, eIF6 was reported to be a component of a large TRBP-containing complex involved in miRNA-mediated post-transcriptional silencing [19]. However, the importance of eIF6 in miRNA-mediated silencing remains controversial [21]. In this study, we report that, although RACK1 is involved in miRNA-mediated silencing, it did not influence of translational machinery complexes containing eIF6, but instead appears to recruit mature miRNAs to the RISC.

The importance of RACK1 in regulating miRNA function was independently reported during the preparation of this manuscript [26]. Similar to our cases, they reported that RACK1 is required for miRNA function; however, the mechanism they reported differed from ours. They found that RACK1 contributes to the recruitment of RISC to the site of translation through binding with Ago2. While we could not detect the effects of RACK1 on miRNA-mediated translational repression as described above, our results were based on the use of synthesized mature miRNAs, which appear functionally Ago2-independent. Due to the fact that we also detected binding between RACK1 and Ago2, their proposed mechanism remains a possibility [26]. In addition, the importance of these diverse mechanisms might be dependent on different types of miRNAs. For example, the maturation of miRNAs used in our study, i.e., miR122, miR140, and miR185, is KSRP-independent [29]. Taking these points into consideration, in the future it may be necessary to determine if RACK1 is involved in different types of miRNA function under the same mechanisms, using various kinds of miRNAs.

We found that RACK1 interacts with KSRP particularly when Dicer is overexpressed. KSRP is a key mediator of AU-rich element-containing mRNA degradation [27,28] that has also been reported to bind to and promote the maturation of a subset of miRNA precursors [29]. In our study, however, maturation of miRNAs examined was preserved and the transfected synthetic miRNAs functioned appropriately in RACK1-knockdown cells. Moreover, levels of miRNAs in Ago2-containing complexes were

decreased in RACK1-knockdown cells. Based on these observations, we speculate that RACK1 is only involved in the recruitment of mature miRNAs to RISCs from miRNA maturation to the point at which they exert their effects *in vivo*. Although the precise mechanisms by which RACK1 contributes to the recruitment of miRNAs to RISCs and the biological significance of its binding to KSRP remains to be determined, these results suggest that RACK1 may regulate miRNA function as a component of a KSRP complex and during the maturation of miRNAs and their recruitment to RISCs.

Translationally repressed mRNA accumulates in discrete cytoplasmic foci known as p-bodies [24] or in another class of cytoplasmic aggregates, stress granules [32]. Although RACK1 has been reported to mediate stress granule formation [33], no change in the localization of p-bodies or expression of the p-body marker GW182 was detected in RACK1-knockdown cells in the present study. Additionally, no interaction between p-bodies and RACK1 was observed. We thus conclude that RACK1 does not produce p-body-related effects in the miRNA pathway.

Retroviral insertion-mediated random gene disruption screening in this study identified several genes involved in miRNA function. Functional genomics approaches involving RNAi libraries have recently been used to identify genes involved in certain functional pathways [34–37]. However, RNAi libraries may not be suitable for identifying genes involved in miRNA- or siRNA-related pathways, because they affect the pathways being examined. Thus, random gene disruption, as used here, may be a useful alternative option for the functional screening of such genes.

While identified genes here did not include well-known components of the miRNA pathway such as Dicer and Ago2, these genes may be critical for cell survival, which would make their selection by survival screening impossible. Alternatively, it may be that the screening required a greater number of cells. Nonetheless, we newly identified six genes that may potentially be involved in miRNA function. Of the genes identified, two, RPS23 and RPL11, are ribosome-related molecules, encoding 40S and 60S subunit proteins, respectively. In view of the fact that one of RACK1's roles is as a mediator of the synthesis of 80S ribosomes (composed of 40S and 60S subunits) [18], these results may suggest the importance of the ribosomal machinery in miRNA function.

Consistent with recent evidence linking global microRNA depletion with oncogenesis [12,30], RACK1 expression was found to be reduced in HCC. Because RACK1 staining in non-cancerous liver tissues was stronger than that in other tissues, the involvement of RACK1 in physiological functions may be more relevant in the liver. These results suggest that the miRNA functional impairment plays an important role in oncogenesis in the liver and/or the maintenance of oncogenicity in HCC, similar to the deficiency of miRNA expression [11].

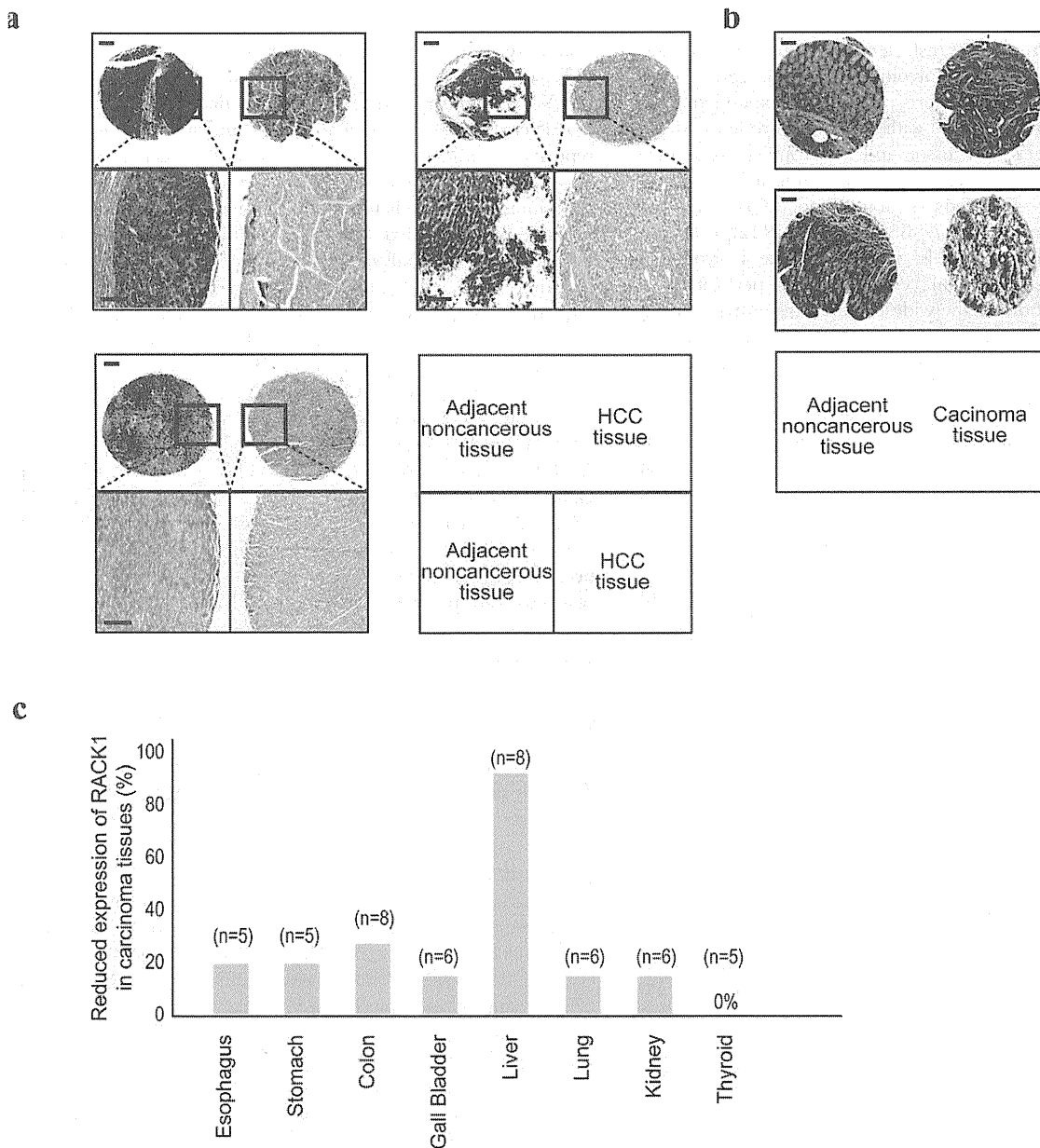


**Figure 5. RACK1 expression is reduced in HCC. A,** Immunohistochemical analysis of RACK1 protein expression in HCC and non-cancerous surrounding tissues. While strong staining was observed in the cytoplasm of hepatocytes in non-cancerous liver tissues (upper left (one panel)), HCC cells were stained more weakly (upper right). Lower panels: magnified images of the highlighted regions in the corresponding upper panels. Three representative cases are shown. Scale bar, 500  $\mu$ m. **B,** Comparable expression of RACK1 in colon carcinoma tissues (right images) and non-cancerous surrounding tissues (left). Two representative cases are shown. Scale bar, 500  $\mu$ m. **C,** Comparison of RACK1 staining in cancers and healthy surrounding tissues. Eight types of cancers were examined. Percentages of cases in which RACK1 expression was lower in cancerous tissues than in healthy tissues were calculated. The number of cases of each type of cancer studied is indicated. doi:10.1371/journal.pone.0024359.g005

**Materials and Methods**

**Cell culture**

Huh7 and PLC/PRF/5 cells were obtained from the Japanese Collection of Research Bioresources (JCRB, Osaka, Japan). 293T cells were obtained from the American Type Culture Collection (ATCC, Rockville, MD). Cells were maintained in Dulbecco’s modified Eagle’s medium (DMEM) supplemented with 10% fetal bovine serum (FBS). Stable cell lines derived from Huh7 and PLC/PRF/5 cells were established by retroviral or lentiviral infection. Clones were selected through the addition of 6  $\mu$ g/mL

puromycin, 400  $\mu$ g/mL hygromycin, or 5  $\mu$ g/mL blasticidin to the culture medium, unless otherwise specified.

**Random gene disruption**

The use of a pDisrupt retroviral vector carrying a blasticidin resistance gene for random gene disruption has been described previously [13]. Retroviruses were produced by transfection of the retroviral vector into virus-packaging Platinum A cells (Orbigen, San Diego, CA). Then, 48 h after transfection, the supernatants were harvested and viruses collected. To prepare reporter cell



lines, Huh7 cells were first transfected with pBSII-Hygro and selected on hygromycin. To avoid random integration in polyclonal cells, single clones were picked and expanded. The selected clones were then infected with MIR122-puro lentiviruses, which express a miR122 precursor and a puromycin resistance gene, and selected on puromycin. Again, several individual clones were isolated and expanded separately to avoid random integration. Using selected Huh7-pBSII-Hygro-miR122 cells and parental Huh7-pBSII-Hygro cells, titration of the hygromycin concentration required for total cell killing was performed to determine the clone showing the widest differences in hygromycin concentration (i.e., the clone in which expression of the hygromycin resistance gene was most effectively suppressed by miR122). Next, this clone was infected with retroviruses at low multiplicities of infection (~0.01) to achieve random gene disruption and then treated with blasticidin. Blasticidin-resistant cells carry viruses inserted in functional genes (otherwise, the blasticidin resistant gene cannot be expressed). Then, hygromycin was added to select hygromycin resistant cells, which potentially have impaired miR122 function as a result of gene disruption (which itself results in impaired suppression of hygromycin resistance gene expression). Such clones were picked and 3'-rapid amplification of cDNA ends (RACE) analysis of the mRNAs fused with the blasticidin gene used to identify the disrupted gene in each clone.

### 3'-RACE

We infected ~106 Huh7-pBS-Hygro-miR122 cells and obtained ~104 blasticidin-resistant clones. After selection, ten surviving clones were obtained. The endogenous gene sequence fused with the blasticidin gene was amplified by 3'-RACE. Total RNA was isolated and reverse transcribed using an RT primer (5'-CCA GTG AGC AGA GTG ACG AGG ACT CGA GCT CAA GC (T)<sub>17</sub>-3'). A nested PCR was performed using primers P0/Q0 (5'-GGT GTC GAC AGG TGC TTC TC-3'/5'-CCA GTG AGC AGA GTG ACG-3') and P1/Q1 (5'-CTG GGA TCA AAG CGA TAG TG-3'/5'-GAG GAC TCG AGC TCA AGC-3'). P0 and P1 anneal to sequences in the blasticidin resistance gene and Q0 and Q1 to the anchor sequences of the RT primer. The PCR fragments were finally subcloned into a TA-cloning vector (Invitrogen, Carlsbad, CA) and sequenced.

### Plasmids

A pBSII-Hygro plasmid containing miR122REs in its 3'-UTR was generated from pGL4-Hygro, purchased from Promega (Madison, WI). Synthetic oligonucleotides containing two tandem miR122-responsive elements were annealed and inserted in the 3'-UTR of this plasmid's hygromycin resistance gene (at the PmeI site). The primer used was 5'-AAA CAC *AAA CAC CAT TGT CAC ACT CCA* AAT TAC *AAA CAC CAT TGT CAC ACT CCA* CTC GAG-3' (miR122-responsive sequences are shown in italics). Next, the gene cassette (containing an SV40 promoter, the hygromycin resistance gene, the miR122 responsive elements and polyA sequences) was excised using BamHI and SalI, and was inserted into pBlueScript II at the same restriction sites. pMIR-122-puro was constructed by replacing the eGFP gene of pMIRH122PA (System Biosciences, Mountain View, CA) at the FseI site by a puromycin resistance gene, which was PCR-amplified using pCDH-EF1 $\alpha$ -puro (System Biosciences) as a template. The following primers were used: 5'-GGC CGG CCG CAT GAC GAG TAC AAG CCC AC-3' and 5'-GGC CGG CCT CAG GCA CCG GGC TTG CGG GT-3'. pcDNA3-myc-RACK1 was used to achieve RACK1 overexpression. Two constructs targeting different RACK1 sequences, pSIH-H1-RACK1shRNA and

pSuper.retro-RACK1 shRNA (both provided by Prof. Takekawa [33]), were used to achieve RACK1 knockdown. pSIH-H1-GFP shRNA was constructed as a control, as described previously [38]. To determine the effect of miR-122 on natural gene targets, a reporter plasmid (CatA-Luc) with natural 3'-UTR sequences of the CATT1 (cationic amino-acid transporter (CAT-1)) gene containing three predicted miR-122 binding sites was used. This plasmid was provided by Prof. W. Filipowicz [22]. Reporter plasmids used to analyze miRNA function were constructed by inserting annealed synthetic primers containing two tandem sequences complementary to each miRNA into the 3'-UTR of the firefly luciferase gene at the FseI site, driven by the CMV promoter (pGL3-basic; Promega). The following primers were used: miR-122, 5'-ACA AAC ACC ATT GTC ACA CTC CAA CTT CAC CCA ACC ATT GTC ACA CTC CAC TCG AGC CGG-3'; miR-140-5p, 5'-CTA CCA TAG GGT AAA ACC ACT GAA TTC TAC CAT AGG GTA AAA CCA CTG CTC GAG CCG G-3'; miR-185, 5'-TCA GGA ACT GCC TTT CTC TCC AAA TTT CAG GAA CTG CCT TTC TCT CCA CTC GAG CCG G-3'. The flag-tagged Dicer-expressing plasmid has been described previously [39]. MiR precursor overexpressing plasmids were purchased from System Biosciences.

### Transfection

Plasmid transfection was performed using FuGENE6 (Boehringer Mannheim, Mannheim, Germany) according to the manufacturer's protocol [40]. Synthetic mature miRNA oligonucleotides (miNatural, CosmoBio, Tokyo, Japan) were transfected using TransMessenger Transfection Reagent (Qiagen, Hilden, Germany).

### Antibodies

The following antibodies were used in Western blotting analyses: anti-Dicer (SAB4200087; Sigma, St. Louis, MO), anti-TRBP2 (SAB4200087; Sigma), anti- $\beta$ -actin (A5316; Sigma), anti-Ago2 (#015-22031; Wako, Osaka, Japan), anti-Gemin3 (DDX20) (SC-57007; Santa Cruz Biotechnology, Santa Cruz, CA), anti-Gemin4 (H00050628; Abnova, Taipei, Taiwan), anti-eIF4E (#9742; Cell Signaling Technology, Danvers, MA), anti-eIF6 (D16E9; Cell Signaling Technology), anti-KSRP (A302-021A; Bethyl, Montgomery, TX), anti-GW182 (MBL Nagoya, Japan), anti-Drosha (#3364; Cell Signaling Technology), anti-DGCR8 (SAB 4200088; Sigma), anti-Ago1 (clone1F2; Wako, Osaka, Japan), anti-Ago3 (SAB2104518; Sigma), anti-Ago4 (SAB2104338; Sigma), anti-Lamin B (SC-20682; Santa Cruz Biotechnology), anti-GAPDH (clone 3C2; Abnova), and anti-myc (Santa Cruz Biotechnology). An Atlas anti-RACK1 antibody was used in immunohistochemical analyses (HPA021676; Sigma).

### Western blotting

Cell extract protein concentrations were measured using a DC Protein Assay Kit (Bio-Rad, Hercules, CA). Total protein (30  $\mu$ g) was resolved by sodium dodecyl sulfate- polyacrylamide gel electrophoresis (SDS-PAGE) and then transferred to Hybond-P polyvinylidene difluoride (PVDF) membranes (Amersham Pharmacia Biotech, Little Chalfont, Buckinghamshire, UK). Membranes were sequentially incubated with primary antibody and horseradish peroxidase-conjugated secondary antibody. Bound antibody was detected using ImmunoStar reagents (Wako) [41].

### Cell fractionation

To separate cytoplasmic and nuclear protein fractions, a ProteoExtract subcellular fractionation kit (Calbiochem-EMD Biosciences, San Diego, CA) was used according to the manufacturer's



protocol. To confirm the identities of the subcellular fractions, Lamin B was blotted for the nuclear fraction and GAPDH for the cytoplasmic fraction.

### Immunocytochemistry

To determine the localization of p-bodies, cells growing on two-well chamber slides were fixed with 4% paraformaldehyde and permeabilized with 0.5% Triton-X100. Fixed cells were then probed with an anti-GW182 antibody for 1 h after blocking with 5% normal goat serum for 30 min. They were then treated with an Alexa Fluor 555-conjugated goat anti-rabbit secondary antibody (Invitrogen) for 30 min. Slides were mounted using VectaShield with DAPI (Vector Labs, Burlingame, CA). Numbers of p-bodies in the cells were determined in three independent views, and the average number or p-bodies per cell calculated. Similar procedures were applied to determine KSRP and Ago2 intracellular localization, except that anti-KSRP and anti-Ago2 were used as first antibodies, and Alexa Fluor 555-conjugated goat anti-rabbit antibody and Alexa Fluor 488-conjugated anti-mouse antibody were used as secondary antibodies.

### Immunohistochemistry

Tissue arrays containing multiple organ carcinoma tissues and matched adjacent non-cancerous tissues (1.5 cm apart; #MC501 and #MC962) were purchased from US Biomax (Rockville, MD). Slides were incubated at 65°C for 1 h and deparaffinized. Endogenous peroxidase activity was blocked through incubation in 3% hydrogen peroxide buffer for 30 min. Antigen retrieval was achieved by incubating the slides at 89°C in 10 mM sodium citrate buffer (pH 6.0) for 30 min. To minimize non-specific background staining, slides were blocked in 5% normal goat serum (Dako, Glostrup, Denmark) for 10 min at room temperature. A primary anti-RACK1 antibody or anti-KSRP antibody, diluted 1:50 in Antibody Diluent (Dako), was applied for 1 h at room temperature. Slides were then incubated with an anti-mouse horseradish peroxidase-conjugated secondary antibody (Nichirei Bioscience, Tokyo, Japan) for 1 h. Bound antibody was visualized by incubation in 3,3'-diaminobenzidine (Nichirei Bioscience; diluted in buffered substrate) for 5 min. The slides were finally counterstained with hematoxylin, dehydrated with ethanol, and mounted using Clarion mounting medium (Biomedica, Foster City, CA).

### Luciferase assay

Luciferase activity were measured using a Dual Luciferase Reporter Assay System (Promega) in conjunction with a Lumat LB9507 luminometer (EG&G Berthold, Bad Wildbad, Germany). pRL-TK, a control plasmid carrying the Renilla reniformis (sea pansy) luciferase gene, driven by the herpes simplex virus thymidine kinase promoter (Toyo Ink, Tokyo, Japan), was used as an internal control. Relative luciferase signals were calculated by dividing firefly luciferase activity by that of the internal control (sea pansy luciferase) (unless otherwise specified). All experiments were performed at least twice (each time in triplicate).

### Lentiviruses and transduction

293T cells were transfected with pPACKH1 Packaging Plasmid Mix (System Biosciences) and pCDH (as a negative control), pSIH-H1-RACK1shRNA, or pMIR122-puro. After 2 days, supernatants were collected and the viruses concentrated using PEG-it Virus Precipitation Solution (System Biosciences) according to the manufacturer's protocol. Lentiviral particles expressing

shRNAs specific for Ago2 (sc-44409) and KSRP (sc-44831) were purchased from Santa Cruz Biotechnology. Polybrene (Millipore, Billerica, MA) was used in lentiviral particle infection.

### miRNA isolation, quantitation, and RIP assay

A Mir-X miRNA qRT-PCR SYBR Kit (Clontech, Mountain View, CA) was used in accordance with the manufacturer's protocol to measure levels of different miRNAs in cells. Total RNA was isolated from cells and tissues using the TRIzol reagent (Invitrogen). Levels of U6 snRNA were used in the normalization of cellular miRNA levels. Relative expression levels were calculated by the  $\Delta\Delta CT$  method:  $\Delta\Delta CT = \Delta CT_{miRNA} - \Delta CT_{U6}$ . To purify miRNAs from Ago2-containing RISC-associated miRNP complexes, miRNA fractions were isolated using the Human Ago2 MicroRNA Isolation Kit (Wako), using antibodies raised against Ago2. The following primers were used in quantitative PCR analyses: miR122, 5'-TGG AGT GTG ACA ATG GTG TTT G-3'; and miR-185, 5'-TGG AGA GAA AGG CAG TTC CTG A-3'.

### Immunoprecipitation

Huh7 cells were transfected with pcDNA3 (negative control) or myc-tagged RACK1-expressing plasmid with or without Dicer-expressing plasmid. When required, cell lysates were incubated at room temperature with RNase A (10  $\mu$ g/mL; Promega) for 30 min. Cell extracts were prepared using immunoprecipitation buffer (50 mM Tris-HCl (pH 7.5), 150 mM NaCl, 0.1% NP-40, 1 mM EDTA, 0.25% gelatin, 0.02% sodium azide, 100  $\mu$ g/mL phenylmethylsulfonyl fluoride, 1  $\mu$ g/mL aprotinin). Myc-tagged RACK1 was precipitated through incubation with anti-myc agarose (#SC-40; Santa Cruz Biotechnology) for 8 h. Anti-KSRP antibodies and Protein A/G Sepharose (#SC-2003; Santa Cruz Biotechnology) were used for endogenous KSRP precipitation. To immunoprecipitate endogenous RACK1 protein, anti-RACK1 antibodies and Protein A/G Sepharose were used. After being washed four times, the precipitated proteins were analyzed by Western blotting using the indicated antibodies. Five percent of each cell lysate was used as "input."

### Statistical analysis

Statistically significant differences between groups were identified using Student's t-test (when variances were equal) or Welch's t-test (when variances were not equal).

### Supporting Information

**Figure S1 miRNA maturation was not impaired in RACK1-knockdown cells.** Total RNA was isolated from control and RACK1-knockdown cells. Levels of mature miR22, miR140-5p, miR140-3p, and miR185, all of which are relatively abundant miRNAs in liver cells, were measured and normalized to the level of U6 snRNA. Relative ratios were calculated by adjusting the value for each miRNA in control cells to 1. Data represent the mean  $\pm$  SD of six independent experiments. (TIF)

**Figure S2 Synthetic mature miRNAs were functional in Ago2-knockdown cells.** **A**, Ago2-knockdown (Ago2 KD) Huh7 cells were established by shRNA-expressing lentiviral infection. **B**, Artificial synthetic miRNA oligonucleotides function normally in Ago2-knockdown Huh7 cells. Control and Ago2-knockdown (Ago2 KD) cells were transfected with miR122 or miR185 reporter plasmids with corresponding synthetic mature miRNA oligonucleotides. Values were normalized to those

obtained from cells transfected with control synthetic oligonucleotides, which were set to 1. Data represent the mean  $\pm$  SD of three independent experiments. \*,  $p < 0.05$ .

(TIF)

**Figure S3 RACK1 binds to KSRP.** Huh7 cells were transiently transfected with a control vector or a myc-tagged RACK1-expressing plasmid, with or without a Flag-tagged Dicer-expressing plasmid. Endogenous KSRP was immunoprecipitated using anti-KSRP with Protein A/G Sepharose. Normal mouse IgG was used as a control for immunoprecipitation. Co-precipitated proteins were blotted using antibodies against myc tag. Five percent of the total cell lysates was loaded as “input.” Representative results from two independent experiments are shown.

(TIF)

**Figure S4 Coimmunoprecipitation of endogenous KSRP and Ago2 with myc-RACK1 is insensitive to RNase A treatment.** Huh7 cells were transiently transfected with a control vector or a myc-tagged RACK1-expressing plasmid. Myc-tagged RACK1 was immunoprecipitated using anti-myc antibody conjugated to agarose. Normal mouse IgG was used as a control for immunoprecipitation. Coprecipitated proteins were blotted using antibodies against the indicated proteins. Five percent of the total cell lysate was loaded as “input.” Representative results from two independent experiments are shown.

(TIF)

**Figure S5 RACK1 may be involved in the recruitment of mature miRNAs to the RISC.** Mature miRNA levels were measured in RNA samples isolated from Ago2-containing complexes from control Huh7 (NC) cells and RACK1-knockdown (siRACK1) cells. miRNA levels were calculated as relative ratios. Data represent the mean  $\pm$  SD of six independent experiments. \*  $p < 0.05$ .

(TIF)

**Figure S6 KSRP is not required for RISC activity.** **A**, KSRP-knockdown Huh7 cells were established by shRNA-expressing lentiviral infection. **B**, Artificial synthetic miRNA oligonucleotides function normally in KSRP-knockdown Huh7 cells. Control

and Ago2-knockdown cells were transfected with miR122 or miR185 reporter plasmids with corresponding synthetic mature miRNA oligonucleotides. Values were normalized to those obtained from cells transfected with control synthetic oligonucleotides, which were set to 1. Data represent the mean  $\pm$  SD of three independent experiments. \*,  $p < 0.05$ .

(TIF)

**Figure S7 KSRP does not bind with Ago2.** Endogenous KSRP was immunoprecipitated using anti-KSRP with Protein A/G Sepharose. Normal rabbit IgG was used as a control for immunoprecipitation. Co-precipitated proteins were blotted using antibodies against Ago2.

(TIF)

**Figure S8 The levels of KSRP expression are high in liver tissues.** **A**, Immunohistochemical analysis of KSRP protein expression in hepatocellular carcinoma (HCC) and non-cancerous surrounding tissues. Lower panels: magnified images of the highlighted regions in the corresponding upper panels. Three representative cases are shown. For a comparison, the sections used here were almost the same parts used for determining RACK1 expression in Fig. 5. Scale bar, 500  $\mu$ m. **B**, Relatively low expression levels of KSRP both in colon carcinoma tissues (right images) and non-cancerous surrounding tissues (left). Two representative cases are shown. Again, for a comparison, the sections used here were almost the same parts used for determining RACK1 expression in Fig. 5. Scale bar, 500  $\mu$ m.

(TIF)

## Acknowledgments

We thank Prof. J. Han, Dr. K. Ono, and Prof. W. Filipowicz for providing the pDisrupt and CatA-Luc plasmids.

## Author Contributions

Conceived and designed the experiments: M. Otsuka M. Omata K. Koike. Performed the experiments: M. Otsuka AT TY K. Kojima TK CS MT HY. Analyzed the data: HY. Contributed reagents/materials/analysis tools: MT. Wrote the paper: M. Otsuka M. Omata K. Koike.

## References

- Gregory R, Chendrimada T, Cooch N, Shiekhattar R (2005) Human RISC couples microRNA biogenesis and posttranscriptional gene silencing. *Cell* 123: 631–640.
- Bartel D (2004) MicroRNAs: genomics, biogenesis, mechanism, and function. *Cell* 116: 281–297.
- Bartel D (2009) MicroRNAs: target recognition and regulatory functions. *Cell* 136: 215–233.
- Krol J, Loedige I, Filipowicz W (2010) The widespread regulation of microRNA biogenesis, function and decay. *Nat Rev Genet* 11: 597–610.
- Siomi H, Siomi M (2010) Posttranscriptional regulation of microRNA biogenesis in animals. *Mol Cell* 38: 323–332.
- Jackson R, Standart N (2007) How do microRNAs regulate gene expression? *Sci STKE* 2007: re1.
- Chekulaeva M, Filipowicz W (2009) Mechanisms of miRNA-mediated post-transcriptional regulation in animal cells. *Curr Opin Cell Biol* 21: 452–460.
- Volinia S, Calin GA, Liu CG, Ambs S, Cimmino A, et al. (2006) A microRNA expression signature of human solid tumors defines cancer gene targets. *Proc Natl Acad Sci U S A* 103: 2257–2261.
- Kumar MS, Lu J, Mercer KL, Golub TR, Jacks T (2007) Impaired microRNA processing enhances cellular transformation and tumorigenesis. *Nat Genet* 39: 673–677.
- Lu J, Getz G, Miska E, Alvarez-Saavedra E, Lamb J, et al. (2005) MicroRNA expression profiles classify human cancers. *Nature* 435: 834–838.
- Sekine S, Ogawa R, Ito R, Hiraoka N, McManus MT, et al. (2009) Disruption of Dicer1 induces dysregulated fetal gene expression and promotes hepatocarcinogenesis. *Gastroenterology* 136: 2304–2315.e2301–2304.
- Melo SA, Ropero S, Moutinho C, Aaltonen LA, Yamamoto H, et al. (2009) A TARBP2 mutation in human cancer impairs microRNA processing and DICER1 function. *Nat Genet* 41: 365–370.
- Wang X, Ono K, Kim S, Kravchenko V, Lin S, et al. (2001) Metaxin is required for tumor necrosis factor-induced cell death. *EMBO Rep* 2: 628–633.
- Ono K, Wang X, Han J (2001) Resistance to tumor necrosis factor-induced cell death mediated by PMCA4 deficiency. *Mol Cell Biol* 21: 8276–8288.
- Kim S, Ha S (2010) Phenotype based functional gene screening using retrovirus-mediated gene trapping in quasi-haploid RAW 264.7 cells. *Methods Mol Biol* 634: 331–342.
- Landgraf P, Rusu M, Sheridan R, Sewer A, Iovino N, et al. (2007) A mammalian microRNA expression atlas based on small RNA library sequencing. *Cell* 129: 1401–1414.
- Nilsson J, Sengupta J, Frank J, Nissen P (2004) Regulation of eukaryotic translation by the RACK1 protein: a platform for signalling molecules on the ribosome. *EMBO Rep* 5: 1137–1141.
- Ceci M, Gaviraghi C, Gorrini C, Sala L, Offenhäuser N, et al. (2003) Release of eIF6 (p27BBP) from the 60S subunit allows 80S ribosome assembly. *Nature* 426: 579–584.
- Chendrimada T, Finn K, Ji X, Baillat D, Gregory R, et al. (2007) MicroRNA silencing through RISC recruitment of eIF6. *Nature* 447: 823–828.
- Kiriakidou M, Tan G, Lamprinak S, De Planell-Saguer M, Nelson P, et al. (2007) An mRNA m7G cap binding-like motif within human Ago2 represses translation. *Cell* 129: 1141–1151.
- Eulalio A, Huntzinger E, Izaurralde E (2008) GW182 interaction with Argonaute is essential for miRNA-mediated translational repression and mRNA decay. *Nat Struct Mol Biol* 15: 346–353.
- Bhattacharyya S, Habermacher R, Martine U, Closs E, Filipowicz W (2006) Relief of microRNA-mediated translational repression in human cells subjected to stress. *Cell* 125: 1111–1124.
- Liu J, Rivas F, Wohlschlegel J, Yates Jr., Parker R, et al. (2005) A role for the P-body component GW182 in microRNA function. *Nat Cell Biol* 7: 1261–1266.
- Eulalio A, Tritschler F, Izaurralde E (2009) The GW182 protein family in animal cells: new insights into domains required for miRNA-mediated gene silencing. *RNA* 15: 1433–1442.

25. Mourelatos Z, Dostie J, Paushkin S, Sharma A, Charroux B, et al. (2002) miRNPs: a novel class of ribonucleoproteins containing numerous microRNAs. *Genes Dev* 16: 720–728.
26. Jannot G, Bajan S, Giguère NJ, Bouasker S, Banville IH, et al. (2011) The ribosomal protein RACK1 is required for microRNA function in both *C. elegans* and humans. *EMBO Rep* 12: 581–586.
27. Chou CF, Mulky A, Maitra S, Lin WJ, Gherzi R, et al. (2006) Tethering KSRP, a decay-promoting AU-rich element-binding protein, to mRNAs elicits mRNA decay. *Mol Cell Biol* 26: 3695–3706.
28. Gherzi R, Lee KY, Briata P, Wegmüller D, Moroni C, et al. (2004) A KH domain RNA binding protein, KSRP, promotes ARE-directed mRNA turnover by recruiting the degradation machinery. *Mol Cell* 14: 571–583.
29. Trabucchi M, Briata P, Garcia-Mayoral M, Haase A, Filipowicz W, et al. (2009) The RNA-binding protein KSRP promotes the biogenesis of a subset of microRNAs. *Nature* 459: 1010–1014.
30. Martello G, Rosato A, Ferrari F, Manfrin A, Cordenonsi M, et al. (2010) A MicroRNA targeting dicer for metastasis control. *Cell* 141: 1195–1207.
31. Yoon S, Kim J, Oh J, Jeon Y, Lee D, et al. (2006) Gene expression profiling of human HBV- and/or HCV-associated hepatocellular carcinoma cells using expressed sequence tags. *Int J Oncol* 29: 315–327.
32. Kedersha N, Anderson P (2007) Mammalian stress granules and processing bodies. *Methods Enzymol* 431: 61–81.
33. Arimoto K, Fukuda H, Imajoh-Ohmi S, Saito H, Takekawa M (2008) Formation of stress granules inhibits apoptosis by suppressing stress-responsive MAPK pathways. *Nat Cell Biol* 10: 1324–1332.
34. Iorns E, Lord C, Turner N, Ashworth A (2007) Utilizing RNA interference to enhance cancer drug discovery. *Nat Rev Drug Discov* 6: 556–568.
35. Ohn T, Kedersha N, Hickman T, Tisdale S, Anderson P (2008) A functional RNAi screen links O-GlcNAc modification of ribosomal proteins to stress granule and processing body assembly. *Nat Cell Biol* 10: 1224–1231.
36. Brass A, Dykxhoorn D, Benita Y, Yan N, Engelman A, et al. (2008) Identification of host proteins required for HIV infection through a functional genomic screen. *Science* 319: 921–926.
37. Birmingham A, Selfors L, Forster T, Wrobel D, Kennedy C, et al. (2009) Statistical methods for analysis of high-throughput RNA interference screens. *Nat Methods* 6: 569–575.
38. Caplen NJ, Parrish S, Imani F, Fire A, Morgan RA (2001) Specific inhibition of gene expression by small double-stranded RNAs in invertebrate and vertebrate systems. *Proc Natl Acad Sci U S A* 98: 9742–9747.
39. Wang Y, Kato N, Jazag A, Dharel N, Otsuka M, et al. (2006) Hepatitis C virus core protein is a potent inhibitor of RNA silencing-based antiviral response. *Gastroenterology* 130: 883–892.
40. Kojima K, Takata A, Vadnais C, Otsuka M, Yoshikawa T, et al. (2011) MicroRNA122 is a key regulator of  $\alpha$ -fetoprotein expression and influences the aggressiveness of hepatocellular carcinoma. *Nat Commun* 2: 338.
41. Takata A, Otsuka M, Kogiso T, Kojima K, Yoshikawa T, et al. (2011) Direct differentiation of hepatic cells from human induced pluripotent stem cells using a limited number of cytokines. *Hepatol Int*.

# Hepatocellular Carcinoma With Extrahepatic Metastasis

## Clinical Features and Prognostic Factors

Koji Uchino, MD<sup>1</sup>; Ryosuke Tateishi, MD, PhD<sup>1</sup>; Shuichiro Shiina, MD, PhD<sup>1</sup>; Miho Kanda, MD, PhD<sup>2</sup>;  
Ryota Masuzaki, MD, PhD<sup>1</sup>; Yuji Kondo, MD, PhD<sup>1</sup>; Tadashi Goto, MD, PhD<sup>1</sup>; Masao Omata, MD, PhD<sup>3</sup>;  
Haruhiko Yoshida, MD, PhD<sup>1</sup>; and Kazuhiko Koike, MD, PhD<sup>1</sup>

**BACKGROUND:** Despite significant advances in the treatment of intrahepatic lesions, the prognosis for patients with hepatocellular carcinoma (HCC) who have extrahepatic metastasis remains poor. The objective of this study was to further elucidate the clinical course and prognostic determinants of patients with this disease. **METHODS:** In total, 342 patients who had HCC with extrahepatic metastasis were enrolled. The metastases were diagnosed at initial presentation with HCC in 28 patients and during follow-up in the remaining patients. The authors analyzed clinical features, prognoses, and treatments and established a scoring system to predict prognosis using a split-sample method with a testing set and a training set. **RESULTS:** The most frequent site of extrahepatic metastasis was the lung followed by lymph nodes, bone, and adrenal glands. These metastases were related directly to death in only 23 patients (7.6%). The median survival after diagnosis of extrahepatic metastasis was 8.1 months (range, 0.03-108.7 months). In univariate analysis of the training set (n=171), performance status, Child-Pugh classification, the number and size of intrahepatic lesions, macroscopic vascular invasion, symptomatic extrahepatic metastases,  $\alpha$ -fetoprotein levels, and complete responses to treatment were associated significantly with prognosis. On the basis of multivariate analysis, a scoring system was developed to predict prognosis that assessed uncontrollable intrahepatic lesions, extent of vascular invasion, and performance status. This scoring system was validated in the testing set (n=171) and produced a concordance index of 0.73. **CONCLUSIONS:** The controllability of intrahepatic lesions and performance status were identified as important prognostic factors in patients with advanced HCC who had extrahepatic metastasis. *Cancer* 2011;117:4475-83. © 2011 American Cancer Society.

**KEYWORDS:** hepatocellular carcinoma, extrahepatic metastasis, clinical course, prognosis.

**Hepatocellular** carcinoma (HCC) is a leading cause of cancer death, and its incidence is particularly high in Asian countries, including Japan.<sup>1,2</sup> HCC usually develops in a liver that already suffers from chronic disease, most notably because of hepatitis B virus (HBV) or hepatitis C virus (HCV) infection.<sup>3</sup> In the past, HCC often was diagnosed only at a far advanced stage, and this was accompanied by a very poor prognosis.<sup>4</sup> However, today, close surveillance with advanced diagnostic modalities on designated high-risk patients has facilitated the detection of HCC at a much early stage. Together with the considerable advances in treatment for HCC, such as surgical resection, percutaneous ablation, transcatheter arterial chemoembolization (TACE), and liver transplantation, the survival of HCC patients has improved much in recent years.<sup>5-9</sup>

Primary HCC lesions often can be removed completely when they are detected at an early stage. Although intrahepatic recurrence of HCC is very frequent, recurrent intrahepatic lesions can be treated successfully using modalities applicable to primary lesions. In particular, percutaneous ablation can be performed repeatedly on recurrent intrahepatic lesions even in patients with moderately impaired liver function. Thus, intrahepatic lesions can be kept under control, but extrahepatic metastasis still may arise.<sup>10,11</sup> Extrahepatic metastasis of HCC were once regarded as a terminal event,<sup>12</sup> and coexisting intrahepatic lesions usually are not treated by locoregional therapies like surgical resection or medical ablation.<sup>13</sup> Although systemic chemotherapies sometimes have been attempted, no standard protocols were established until

**Corresponding author:** Haruhiko Yoshida, MD, PhD, Department of Gastroenterology, Graduate School of Medicine, The University of Tokyo, 7-3-1 Hongo, Bunkyo-ku, Tokyo 113-8655, Japan; Fax: (011) 81-3-3814-0021; yoshida-2im@h.u-tokyo.ac.jp

<sup>1</sup>Department of Gastroenterology, Graduate School of Medicine, The University of Tokyo, Tokyo, Japan; <sup>2</sup>Department of Gastroenterology and Hepatology, Kyoundo Hospital, Tokyo, Japan; <sup>3</sup>Yamanashi Prefectural Hospital Organization, Yamanashi, Japan

**DOI:** 10.1002/cncr.25960, **Received:** September 4, 2010; **Revised:** December 27, 2010; **Accepted:** January 3, 2011, **Published online** March 22, 2011 in Wiley Online Library (wileyonlinelibrary.com)

recently.<sup>14,15</sup> In 2 recent, large, randomized controlled trials, it was demonstrated that the multikinase inhibitor sorafenib significantly prolonged survival in patients with advanced HCC, even when the primary lesion was accompanied by extrahepatic metastases; now, sorafenib is widely regarded as the standard treatment for such patients.<sup>16,17</sup> However, the clinical course for patients with extrahepatic metastasis has not yet been fully elucidated, and the prognostic factors remain unclear. This information will be vital when determining whether treatment with sorafenib or other such agents is indicated.

The prognosis for patients with HCC who had extrahepatic metastasis before the availability of sorafenib may represent the natural clinical course for affected patients, because no previous treatments had proven effective. In the current study, we retrospectively analyzed a cohort of these patients to further investigate the clinical features and prognostic factors for HCC with extrahepatic metastasis.

## MATERIALS AND METHODS

### *Patients*

This study was conducted according to the ethical guidelines for epidemiologic research designed by the Ministry of Education, Culture, Sports, Science, and Technology and the Ministry of Health, Labor and Welfare, Japan. The study design was approved by the ethics committee of the host institution. Between 1990 and 2006, a total of 2386 patients with HCC were admitted to the University of Tokyo Hospital. A diagnosis of HCC was confirmed radiologically by hyperattenuation in the arterial phase and washout in the late phase using either contrast-enhanced computed tomography (CT) or magnetic resonance imaging (MRI).<sup>18</sup> Ultrasound-guided tumor biopsies were performed when the diagnostic imaging results were inconclusive. In the current analysis, the follow-up period ended on the date of death or on December 31, 2008. Among the 2386 patients in the total HCC cohort in our hospital, extrahepatic metastases were noted in 28 patients at first hospitalization. In addition, extrahepatic metastases were detected in other 314 patients during follow-up observation. Therefore, we retrospectively analyzed 342 patients in our current study.

### *Diagnosis of Extrahepatic Metastasis and Evaluation of Intrahepatic Lesions*

Screenings for extrahepatic metastases were not performed as part of the routine check-up. Most intra-abdominal metastases were detected on abdominal ultrasonography, CT, or MRI studies that were obtained every 3 to 4

months to evaluate intrahepatic lesions. Pulmonary lesions often were noted on chest x-rays, which were obtained routinely at each admission. Additional examinations, such as bone x-ray, bone scintigraphy, and brain CT or MRI studies, were indicated when symptoms attributable to extrahepatic metastasis appeared. These examinations also were undertaken when the HCC-specific tumor markers  $\alpha$ -fetoprotein (AFP), lens culinaris agglutinin-reactive fraction of AFP (AFP-L3), or des- $\gamma$ -carboxy prothrombin (DCP) were elevated and the elevation could not be accounted for by status of the intrahepatic lesion. A diagnosis of extrahepatic metastasis from HCC was based on the enhancement pattern observed on contrast-enhanced CT/MRI studies. Positron emission tomography/CT studies were not obtained routinely, because they were not covered by insurance in Japan. When tumor resections were performed, pathologic investigations also were undertaken. Extrahepatic metastasis detected only at autopsy was not considered an event in this study, because we focused primarily on the diagnosis and treatment of this condition in living patients.

We also evaluated viable intrahepatic lesions at the diagnosis of extrahepatic metastasis by using contrast-enhanced CT/MRI. Post-treatment lesions were not considered viable if they were not enhanced by contrast medium. In the current study, vascular invasion was diagnosed radiologically, indicating *macroscopic vascular invasion*. Vascular invasion included invasion to the portal vein, hepatic vein, inferior vena cava, and bile duct.

### *Treatment Responses in Patients With Extrahepatic Metastasis*

In principle, treatment responses were evaluated according to Response Evaluation Criteria in Solid Tumors (RECIST) guidelines.<sup>19</sup> A complete response (CR) was defined as the disappearance of both intrahepatic lesion and extrahepatic metastasis. In addition, we defined a CR as the disappearance of all intratumoral arterial enhancement according to a recently proposed, modified RECIST assessment for HCC.<sup>20</sup> The evaluation was based on imaging results that were obtained at 2 months after the initiation of treatment. CR was confirmed by repeat assessments performed  $\geq 4$  weeks after the criteria for response first were met.

### *Statistical Procedures*

Survival after diagnosis of extrahepatic metastases was defined as the interval from the date of diagnosis to the date of death from any cause or to the last visit before

December 31, 2008. The cumulative survival probability was calculated using the Kaplan-Meier method. The cause of death was investigated meticulously using medical records. To develop a scoring system as a prognostic predictor for patients with extrahepatic metastasis, a split-sample method was applied. Our 342 patient cohort was divided randomly into 2 groups: a training set ( $n = 171$ ) and a testing set ( $n = 171$ ). The clinical data obtained at the diagnosis of extrahepatic metastasis were assessed as predictors of survival using a Cox proportional hazards model in the training set. The following variables were included in this analysis: age, sex, Eastern Cooperative Oncology Group (ECOG) performance status,<sup>21</sup> hepatitis B surface antigen (HBsAg), HCV antibody, Child-Pugh classification, the size and number of intrahepatic lesion(s), the presence of macroscopic vascular invasion, the presence of symptoms of extrahepatic metastasis, HCC-specific tumor marker levels (AFP, AFP-L3, and DCP), and response to treatment. Each variable was assessed first in a univariate analysis, and the variables that reached a  $P$  value  $< .05$  were evaluated in a multivariate analysis with stepwise variable selection using Akaike information criterion (AIC). Then, the ratio of regression coefficients of the final model was determined and was rounded to whole digits for convenience. This scoring system was validated in the test group using the chi-square trend test and the Harrell concordance index (c-index).<sup>22</sup> Data were expressed as the mean  $\pm$  standard deviation unless specified otherwise. All  $P$  values  $< .05$  were considered statistically significant. All analytical procedures were performed with S-plus (version 7.0; Insightful Corp., Seattle, Wash).

## RESULTS

### Patient Background Data

Table 1 indicates that the average age at diagnosis for patients with primary extrahepatic metastasis from HCC was  $66.9 \pm 9.0$  years, and ratio of men to women was 4:1. The distribution of the metastases among patients was the lung in 135 patients (39.5%), lymph node in 117 patients (34.2%), bone in 87 patients (25.4%), adrenal in 30 patients (8.8%), brain in 4 patients (1.2%), spleen in 2 patients (0.6%), and breast in 1 patient (0.3%), for a total of 376 extrahepatic occurrences in 342 patients. Metastases that were detected within 2 weeks after diagnosis of the first metastasis were considered synchronous. Viable, coexisting intrahepatic HCC lesions were identified in 281 patients (82.2%) when the extrahepatic metastasis

**Table 1.** Patient Characteristics at the Diagnosis of Extrahepatic Metastasis ( $n = 342$ )

Variable	No. of Patients (%)
Age: Mean $\pm$ SD, y	66.9 $\pm$ 9.0
Men	270 (78.9)
<b>Performance status</b>	
0-1	314 (91.8)
$\geq 2$	28 (8.2)
<b>Viral infection</b>	
HBsAg, positive	62 (18.1)
Anti HCVAb, positive	268 (78.4)
Both positive	15 (4.4)
Both negative	27 (7.9)
<b>Child-Pugh class</b>	
A	167 (48.8)
B	153 (44.7)
C	22 (6.4)
<b>Status of intrahepatic lesions</b>	
None	61 (17.8)
$\leq 3$ cm and 1-3 lesions	110 (32.2)
$> 3$ cm or $\geq 4$ lesions	171 (50)
Macroscopic vascular invasion, present	65 (19)
<b>Site of extrahepatic metastasis<sup>a</sup></b>	
Lung	135 (39.5)
Lymph node	117 (34.2)
Bone	87 (25.4)
Adrenal gland	30 (8.8)
Brain	4 (1.2)
Spleen	2 (0.6)
Breast	1 (0.3)
Symptoms of extrahepatic metastasis, present	80 (23.4)
AFP $> 400$ ng/mL	158 (46.2)
AFP-L3 $> 15\%$ <sup>b</sup>	169 (64.8)
DCP $> 100$ mAU/mL	196 (57.3)

SD indicates standard deviation; HCVAb, hepatitis C virus antibody; AFP, alpha-fetoprotein; AFP-L3, lens culinaris agglutinin-reactive fraction of AFP; DCP, des-gamma-carboxy prothrombin.

<sup>a</sup>Including overlap.

<sup>b</sup>Missing in 81 patients.

was diagnosed. Intrahepatic vascular tumor invasion was evident in 65 patients (19%) patients: Portal vein invasion was evident in 57 patients, hepatic vein and inferior vena cava invasion was evident in 13 patients, and invasion into the bile duct was evident in 4 patients. The ECOG performance status was 0 in 229 patients, 1 in 85 patients, 2 in 19 patients, 3 in 5 patients, and 4 in 4 patients. Eighty patients (23.4%) had symptoms caused by extrahepatic metastasis, including dyspnea caused by multiple lung metastases; bone fracture, nerve paralysis, and pain caused by bone metastasis; abdominal pain and obstructive jaundice caused by abdominal lymph node metastasis; and disturbance of consciousness caused by bleeding from brain metastasis.

**Table 2.** Treatments Received for Extrahepatic Metastasis in the Study Cohort<sup>a</sup>

Organ	Total No.	No. of Patients (%)					
		Resection	Ablation	TACE	Radiation	Chemotherapy	No Treatment
Lung	135	19 (14.1)	—	1 (0.7)	4 (3)	42 (31.1)	69 (51.1)
Lymph nodes	117	8 (6.8)	5 (4.3)	2 (1.7)	26 (22.2)	27 (23.1)	49 (41.9)
Bone	87	—	3 (3.4)	—	68 (78.2)	2 (2.3)	14 (16.1)
Adrenal gland	30	5 (16.7)	7 (23.3)	11 (36.7)	1 (3.3)	—	6 (20)
Brain	4	—	—	—	2 (50)	—	2 (50)
Spleen	2	1 (50)	—	—	—	—	1 (50)
Breast	1	—	—	—	1 (100)	—	—

TACE indicates transarterial chemoembolization

<sup>a</sup> Including overlap.

### **Treatment of Patients With Extrahepatic Metastasis**

Retrospectively reviewed, the treatments for extrahepatic metastatic lesions in our study cohort were considered only in those patients who had Child-Pugh Class B or better liver function and an ECOG performance status  $\geq 2$  and when intrahepatic lesions, if any, generally were controlled or controllable. Patients also received treatment when they were suffering from symptoms caused by extrahepatic metastasis. Table 2 indicates that these treatments included resection, chemotherapy, irradiation, TACE, and percutaneous ablation.

Surgical resection was undergone by 19 patients who had a lung metastasis (including 13 patients who underwent video-assisted thoracoscopic surgery), 8 patients who had lymph node metastasis, 5 patients who had adrenal metastasis, and 1 patient who has a spleen metastasis. Percutaneous ablation, using either ethanol or radiofrequency, was undergone by 7 patients with adrenal metastasis, 5 patients with lymph node metastasis, and 3 patients with bone metastasis, and TACE was undergone by 11 patients, 2 patients, and 1 patient with of adrenal, lymph node, and lung metastasis, respectively. Irradiation was received by other patients with metastasis as follows: 68 patients with bone metastasis, 26 patients with lymph node metastasis, 4 patients with lung metastasis, 2 patients with brain metastasis, 1 patient with an adrenal metastasis, and 1 patient with a breast metastasis. Systemic chemotherapy was received by an additional 42 patients with lung metastasis, 27 patients with lymph node metastasis, and 2 patients with bone metastasis in our cohort. The most often used chemotherapeutic regimen was cis-diamminedichloroplatinum (CDDP) monotherapy (29 patients) followed by 5-fluorouracil (5-FU) plus interferon (IFN) (24 patients), TS-1 alone (7 patients), CDDP plus 5-FU (6 patients), etoposide alone (6 patients), and TSU-68 (5 patients).

Percutaneous ablation of the intrahepatic lesions, which was indicated only when any extrahepatic lesions had been completely resected or ablated or controlled by irradiation, was performed in 60 patients. TACE treatment of intrahepatic lesions was indicated for patients who had Child-Pugh Class A or B liver function and when the vast majority of the total tumor volume was located in the liver. By using a combination of systemic chemotherapy and/or locoregional therapy to treat intrahepatic lesions, 22 of the patients in our study group achieved a CR as evaluated by the overall response according to RECIST.

### **Prognosis After the Diagnosis of Extrahepatic Metastasis**

In the current study, during the observation period, 301 patients died. The cause of death was related to HCC in 273 patients (90.7%) patients and to liver dysfunction in 15 patients (5%), and death was unrelated to the liver in another 13 patients (4.3%). Extrahepatic metastasis of HCC was related directly to death in 23 patients (7.6%) patients, including 17 deaths from respiratory failure because of a lung metastasis, 5 incidents of cerebral hemorrhage from a brain metastasis, and death in 1 patient who had a bone metastasis and suffered liver failure that caused by hemorrhaging from a bone fracture that was the result of this lesion.

Gastroesophageal varices rupture sometimes became a critical event at the terminal phase of advanced HCC. In the current study, gastroesophageal varices rupture occurred in 25 patients at the end of life. Portal hypertension in these patients was caused either by portal vein tumor thrombus or cirrhosis, which may often coexist and are difficult to discriminate accurately.

The cumulative survival rates at 1 year, 2 years, 3 years, and 5 years after the diagnosis of extrahepatic metastasis in our cohort were 39.3%, 15.3%, 7.4%, and 4%,



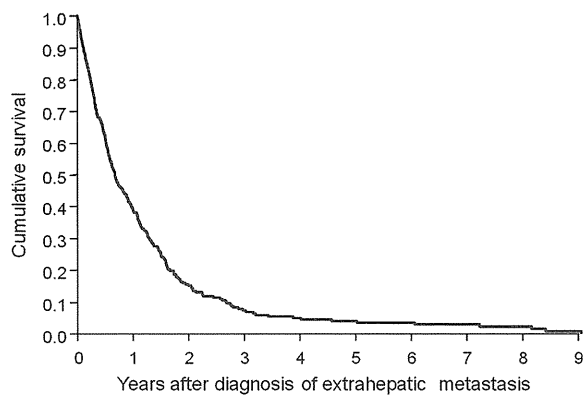


**Figure 1.** Cumulative survival is illustrated for patients with hepatocellular carcinoma who had a diagnosis of extrahepatic metastasis.

respectively (Fig. 1), and the median survival was 8.1 months (range, from 1 day to 108.7 months). The cumulative survival rates at 1 year, 2 year, and 3 years were 48.9%, 21.2%, and 10.6%, respectively, when the patients had received some treatment for extrahepatic metastasis; and the rates were 19%, 2.3%, and 0%, respectively, when no treatment had been indicated.

**Predictors of Prognosis**

Prognostic predictors after the diagnosis of extrahepatic metastasis were analyzed in the training set of 171 patients using a Cox proportional hazards model. These predictors were based on clinical factors that were recorded at diagnosis. In univariate analysis, the following factors were associated significantly with a poor prognosis: performance status, Child-Pugh classification, number and size of intrahepatic lesions, the presence of macroscopic vascular invasion, a symptomatic extrahepatic metastasis, AFP level, and CR to therapy (Table 3). Clinical factors that were statistically significant in univariate analysis were analyzed further in multivariate analysis with a stepwise selection of variables to minimize the AIC. To simplify the scoring system using multivariate analysis, intrahepatic tumor extension was categorized as none, a viable lesion without vascular invasion, or a viable lesion with vascular invasion. Only intrahepatic tumor extension at the diagnosis of extrahepatic metastasis and performance status were selected by a stepwise selection as factors in the final model (Table 4). Scores were assigned to each factor according to the estimated regression coefficient in the final model, and the prognosis score was defined as the sum of each score (Table 5). Our scoring system was vali-

**Table 3.** Predictors of Survival After a Diagnosis of Extrahepatic Metastasis: Univariate Analysis (n = 171)

Variable	$\beta$	HR (95% CI)	P
Age	0.02	1.02 (1.00-1.03)	.12
Men	0.07	1.08 (0.72-1.61)	.72
<b>Performance status</b>			
0		1.00	
1	0.36	1.44 (1.00-2.07)	.05
2	1.08	2.96 (1.29-6.79)	.01
3	2.61	13.5 (3.90-47.04)	<.0001
4	1.07	2.93 (0.40-21.26)	.29
HBsAg positive	-0.17	0.84 (0.53-1.33)	.46
Anti-HCVAb-positive	-0.27	0.76 (0.51-1.15)	.19
<b>Child-Pugh class</b>			
A		1.00	
B	0.37	1.44 (1.03-2.02)	.03
C	0.64	1.90 (0.97-3.69)	.06
<b>Size of intrahepatic lesion, cm</b>			
Absent		1.00	
$\leq 3.0$	0.71	2.04 (1.18-3.51)	.01
$> 3.0$	1.41	4.12 (2.31-7.32)	<.0001
<b>No. of intrahepatic lesion</b>			
Absent		1.00	
1-3	0.67	1.96 (1.16-3.30)	.01
$> 3$	0.93	2.52 (1.55-4.11)	.0002
Macroscopic vascular invasion, present	0.78	2.18 (1.46-3.25)	.0001
Symptom of extrahepatic metastasis, present	0.37	1.45 (1.01-2.09)	.047
AFP $> 400$ ng/mL	0.54	1.71 (1.23-2.39)	.002
AFP-L3 $> 15.0\%$	0.30	1.34 (0.92-1.96)	.12
DCP $> 100$ mAU/mL	0.08	1.09 (0.78-1.51)	.62
Response to treatment, CR <sup>a</sup>	-0.77	0.46 (0.21-1.00)	.049

HR indicates hazard ratio; CI, confidence interval; HBsAg, hepatitis B surface antigen; HCVAb, hepatitis C virus antibody; AFP, alpha-fetoprotein; AFP-L3, lens culinaris agglutinin-reactive fraction of AFP; DCP, des-gamma-carboxy prothrombin; CR, complete response

<sup>a</sup>Response was evaluated using overall responses according to Response Evaluation Criteria in Solid Tumors (RECIST); treatments included locoregional therapy and systemic chemotherapy for both intrahepatic lesions and extrahepatic lesions.

dated using the testing set of 171 patients. A Kaplan-Meier plot was used to illustrate distinct survival curves according to the prognosis score (chi-square linear trend test: *P* thinsp; $< .001$ ) (Fig. 2). The c-index for the scoring system in the testing set was 0.73, thus reflecting good prognostic discrimination (Table 6).

**DISCUSSION**

The prognosis for patients with extrahepatic metastasis of HCC was poor in the current study, consistent with previous reports that the 1-year survival rate is approximately 40% for patients with this disease.<sup>23-27</sup> However, from our current analyses, we observed that extrahepatic

**Table 4.** Predictors of Survival After a Diagnosis of Extrahepatic Metastasis: Multivariate Analysis (n = 171)

Variable	$\beta$	HR (95% CI)	P
<b>Intrahepatic viable lesion</b>			
None		1.00	
Without macroscopic vascular invasion	0.67	1.96 (1.21-3.18)	.006
With macroscopic vascular invasion	1.31	3.70 (2.08-6.57)	<.0001
<b>Performance status</b>			
0		1.00	
1	0.30	1.36 (0.94-1.96)	.11
2	1.11	3.05 (1.32-7.06)	.009
3-4	1.78	5.94 (2.09-16.9)	.0008

HR indicates hazard ratio; CI, confidence interval.

**Table 5.** Scoring System to Predict Survival in Patients With HCC and Extrahepatic Metastasis

Variable	Score
<b>Intrahepatic viable lesion</b>	
None	0
Present without macroscopic vascular invasion	1
Present with macroscopic vascular invasion	2
<b>Performance status</b>	
0-1	0
2	2
3-4	3

metastasis was not the direct cause of death in the majority of affected patients: the exceptions included respiratory failure from a bilateral lung metastasis and cerebral hemorrhage as a result of a brain metastasis, which accords with a previous report.<sup>28</sup> Hence, the presence of extrahepatic metastasis is an indicator of the aggressiveness of the primary HCC as a whole rather than an independent prognostic determinant.

In contrast to extrahepatic metastases, the progression of intrahepatic lesions was identified as the cause of death in 81% of patients in our current cohort, indicating the importance of controlling intrahepatic tumors in patients with HCC whenever possible. Repeated percutaneous ablations or TACE generally are considered for patients with HCC who develop an intrahepatic recurrence.<sup>29,30</sup> Intrahepatic arterial chemotherapy also reportedly is effective against advanced HCC with portal venous tumor invasion.<sup>31</sup> Thus, these locoregional treatments should be considered for intrahepatic lesions in selected patients who have extrahepatic metastasis, although the liver function reservoir should be evaluated cautiously in these patients.

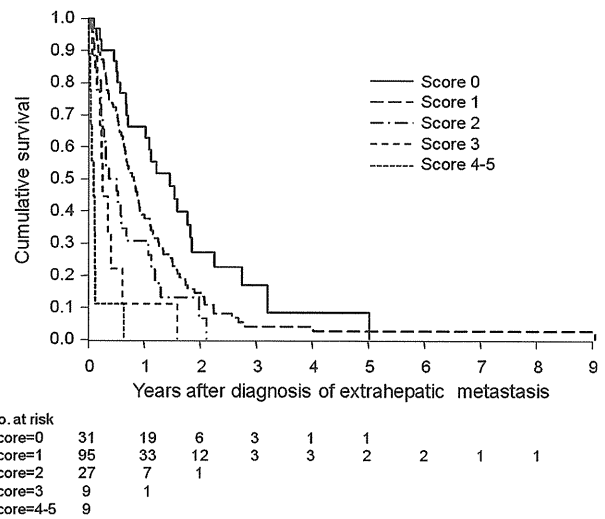


**Figure 2.** Stratified cumulative survival is illustrated for patients with hepatocellular carcinoma who had a diagnosis of extrahepatic metastasis based on prognostic scores. The prognosis for patients in the testing set could be stratified clearly by the scoring system based on an analysis of patients in the training set.

**Table 6.** Median Survival According to Prognostic Scores (n = 171)

Score	No. of Patients	Median Survival, mo
0	31	17.5
1	95	9.7
2	27	6.1
3	9	3.0
4-5	9	1.2

In the current study cohort, patients received treatment for extrahepatic metastasis when their intrahepatic tumor was under control and liver function was maintained. Extrahepatic metastases also were treated when metastasis-related symptoms were strong or when further progression of the metastatic lesions was considered life-threatening. The prognosis was better among the current patients with HCC who received some treatment for their extrahepatic metastasis compared with those who were untreated. However, the contribution of these treatments to the overall prognosis remains unknown, because the patients who received them generally were in better condition. Nevertheless, our current findings indicate that treatments for extrahepatic metastases can be considered in patients who have hepatic lesions under control, because long-term survival was achieved only in those who had received such therapies.

Our current analyses indicated that resection of metastatic lesions produced a satisfactory local response, consistent with previous reports.<sup>32-36</sup> Locoregional therapy for extrahepatic metastasis also was discussed in earlier studies, including irradiation for bone,<sup>37</sup> lymph node,<sup>38</sup> brain,<sup>39</sup> and adrenal<sup>40</sup> metastases; TACE for adrenal metastasis<sup>41</sup>; and percutaneous ablation for adrenal<sup>42</sup> and bone metastases.<sup>43</sup> We also used these methods to treat some patients in our cohort. According to the conventional treatment strategy for solid tumors, the presence of metastatic disease is a contraindication for locoregional therapy, because it is believed that these tumor cells already have spread systemically. However, from the viewpoint of reducing tumor burden, locoregional therapy may be an adequate strategy when the target lesions account for the major portion of the total tumor volume. When resection and other locoregional therapies were contraindicated for extrahepatic metastasis, we sometimes used systemic chemotherapy. However, the overall response rate to conventional chemotherapy in the current study was only 25.4%. The establishment of an effective chemotherapeutic regimen still is needed for these patients, and molecular targeted agents, such as sorafenib,<sup>16,17</sup> are expected to improve their prognosis.

The scoring system we propose in the current study incorporates the presence of intrahepatic lesions, the extent of vascular invasion, and performance status. The progression of an intrahepatic lesion was the major cause of death among our patients, as described above. In patients who had extrahepatic metastases, evaluation of the size and number of intrahepatic lesions often is difficult because of disease progression. From the standpoint of these patients, the proposed scoring system is both simple and convenient. Vascular invasion is 1 of the most important prognostic factors for HCC.<sup>12</sup> Our current results demonstrated that macroscopic vascular invasion is significant even in patients who have extrahepatic metastasis. Performance status, which is an important biologic factor in clinical oncology, also is included in our scoring system.<sup>13</sup> Liver function no doubt is a prognostic determinant for patients with HCC; however, the Child-Pugh classification did not retain significance in our multivariate analysis. This may be because the Child-Pugh class is strongly correlated with performance status, which also includes other significant aspects of cancer biology.

Our current results indicate that the median survival of patients with HCC who have extrahepatic metastases varies widely from within 1 month to 1.5 years and can be discerned using the prognosis factors that were evaluated in

this study. Patients who have a prognostic score  $\geq 2$ , which indicates an estimated median survival  $\geq 6$  months, can be considered for intensive treatment, including surgical procedures. In addition, our scoring system may be used for the enrollment of patients into clinical trials of newly developed agents for which patients with extrahepatic metastasis or vascular invasion may be candidates, although further detailed research will be required to establish such use. We compared the prognosis of patients who were treated in the 1990s and the 2000s and observed no statistical difference between the 2 decades (data not shown). During the study period, newly developed agents, such as sorafenib and drug-eluting beads, were not available in Japan.

There were some limitations in this retrospective cohort study. First, a variety of treatments was provided for various intrahepatic and extrahepatic lesions. Substantial heterogeneity existed in patient background. Second, the proportion of patients who had vascular invasion in our cohort was relatively small despite the presence of extrahepatic metastasis, and this may indicate that the total tumor burden also was relatively small. This may have been because most extrahepatic metastasis in our cohort emerged while treatment for intrahepatic lesions was being repeated. Moreover, the proportion of patients with vascular invasion was not very high, even among the patients who had extrahepatic metastasis at initial presentation. Supposedly, this is because our hospital is a tertiary care center, and patients with an apparent indication for percutaneous ablation were referred to us selectively. Third, the number of patients who had prognostic scores of 3, 4, 5 was not large enough for confirmation, although the linearity of median survival (Table 6) suggests the relevance of the scoring system.

In conclusion, the major cause of death in patients with HCC who have extrahepatic metastases is progression of the intrahepatic HCC lesion. We contend that treatment of intrahepatic lesions should not be contraindicated merely because of the presence of an extrahepatic metastasis. Moreover, radical treatments for extrahepatic metastases may be considered when hepatic lesions are under reasonable control or if the metastasis is accompanied by severe symptoms.

## CONFLICT OF INTEREST DISCLOSURES

The authors made no disclosures.

## REFERENCES

1. Parkin DM, Bray F, Ferlay J, Pisani P. Global cancer statistics, 2002. *CA Cancer J Clin.* 2005;55:74-108.

2. Matsuda T, Marugame T, Kamo K, Katanoda K, Ajiki W, Sobue T. Cancer incidence and incidence rates in Japan in 2003: based on data from 13 population-based cancer registries in the Monitoring of Cancer Incidence in Japan (MCIJ) Project. *Jpn J Clin Oncol*. 2009;39:850-858.
3. Shiratori Y, Shiina S, Imamura M, et al. Characteristic difference of hepatocellular carcinoma between hepatitis B- and C-viral infection in Japan. *Hepatology*. 1995;22(4 pt 1):1027-1033.
4. Okuda K, Ohtsuki T, Obata H, et al. Natural history of hepatocellular carcinoma and prognosis in relation to treatment. Study of 850 patients. *Cancer*. 1985;56:918-928.
5. Arii S, Yamaoka Y, Futagawa S, et al. Results of surgical and nonsurgical treatment for small-sized hepatocellular carcinomas: a retrospective and nationwide survey in Japan. The Liver Cancer Study Group of Japan. *Hepatology*. 2000;32:1224-1229.
6. Shiina S, Tagawa K, Niwa Y, et al. Percutaneous ethanol injection therapy for hepatocellular carcinoma: results in 146 patients. *AJR Am J Roentgenol*. 1993;160:1023-1028.
7. Llovet JM, Real MI, Montana X, et al. Arterial embolisation or chemoembolisation versus symptomatic treatment in patients with unresectable hepatocellular carcinoma: a randomised controlled trial. *Lancet*. 2002;359:1734-1739.
8. Shiina S, Teratani T, Obi S, et al. A randomized controlled trial of radiofrequency ablation with ethanol injection for small hepatocellular carcinoma. *Gastroenterology*. 2005;129:122-130.
9. Mazzaferro V, Regalia E, Doci R, et al. Liver transplantation for the treatment of small hepatocellular carcinomas in patients with cirrhosis. *N Engl J Med*. 1996;334:693-699.
10. Katsyal S, Oliver JH 3rd, Peterson MS, Ferris JV, Carr BS, Baron RL. Extrahepatic metastases of hepatocellular carcinoma. *Radiology*. 2000;216:698-703.
11. Kanda M, Tateishi R, Yoshida H, et al. Extrahepatic metastasis of hepatocellular carcinoma: incidence and risk factors. *Liver Int*. 2008;28:1256-1263.
12. Bruix J, Sherman M. Management of hepatocellular carcinoma. *Hepatology*. 2005;42:1208-1236.
13. Llovet JM, Burroughs A, Bruix J. Hepatocellular carcinoma. *Lancet*. 2003;362:1907-1917.
14. Burroughs A, Hochhauser D, Meyer T. Systemic treatment and liver transplantation for hepatocellular carcinoma: two ends of the therapeutic spectrum. *Lancet Oncol*. 2004;5:409-418.
15. Nowak AK, Chow PK, Findlay M. Systemic therapy for advanced hepatocellular carcinoma: a review. *Eur J Cancer*. 2004;40:1474-1484.
16. Llovet JM, Ricci S, Mazzaferro V, et al. Sorafenib in advanced hepatocellular carcinoma. *N Engl J Med*. 2008;359:378-390.
17. Cheng AL, Kang YK, Chen Z, et al. Efficacy and safety of sorafenib in patients in the Asia-Pacific region with advanced hepatocellular carcinoma: a phase III randomised, double-blind, placebo-controlled trial. *Lancet Oncol*. 2009;10:25-34.
18. Torzilli G, Minagawa M, Takayama T, et al. Accurate pre-operative evaluation of liver mass lesions without fine-needle biopsy. *Hepatology*. 1999;30:889-893.
19. Therasse P, Arbuck SG, Eisenhauer EA, et al. New guidelines to evaluate the response to treatment in solid tumors. European Organization for Research and Treatment of Cancer, National Cancer Institute of the United States, National Cancer Institute of Canada. *J Natl Cancer Inst*. 2000;92:205-216.
20. Lencioni R, Llovet JM. Modified RECIST (mRECIST) assessment for hepatocellular carcinoma. *Semin Liver Dis*. 2010;30:52-60.
21. Oken MM, Creech RH, Tormey DC, et al. Toxicity and response criteria of the Eastern Cooperative Oncology Group. *Am J Clin Oncol*. 1982;5:649-655.
22. Harrell FE Jr, Lee KL, Califf RM, Pryor DB, Rosati RA. Regression modelling strategies for improved prognostic prediction. *Stat Med*. 1984;3:143-152.
23. Shimada M, Takenaka K, Gion T, et al. Prognosis of recurrent hepatocellular carcinoma: a 10-year surgical experience in Japan. *Gastroenterology*. 1996;111:720-726.
24. Ishii H, Furuse J, Kinoshita T, et al. Extrahepatic spread from hepatocellular carcinoma: who are candidates for aggressive anti-cancer treatment? *Jpn J Clin Oncol*. 2004;34:733-739.
25. Uka K, Aikata H, Takaki S, et al. Clinical features and prognosis of patients with extrahepatic metastases from hepatocellular carcinoma. *World J Gastroenterol*. 2007;13:414-420.
26. Yang Y, Nagano H, Ota H, et al. Patterns and clinicopathologic features of extrahepatic recurrence of hepatocellular carcinoma after curative resection. *Surgery*. 2007;141:196-202.
27. Natsuizaka M, Omura T, Akaike T, et al. Clinical features of hepatocellular carcinoma with extrahepatic metastases. *J Gastroenterol Hepatol*. 2005;20:1781-1787.
28. Okusaka T, Okada S, Ishii H, et al. Prognosis of hepatocellular carcinoma patients with extrahepatic metastases. *Hepatogastroenterology*. 1997;44:251-257.
29. Tateishi R, Shiina S, Teratani T, et al. Percutaneous radiofrequency ablation for hepatocellular carcinoma. An analysis of 1000 cases. *Cancer*. 2005;103:1201-1209.
30. Takayasu K, Arii S, Ikai I, et al. Prospective cohort study of transarterial chemoembolization for unresectable hepatocellular carcinoma in 8510 patients. *Gastroenterology*. 2006;131:461-469.
31. Obi S, Yoshida H, Toune R, et al. Combination therapy of intra-arterial 5-fluorouracil and systemic interferon-alpha for advanced hepatocellular carcinoma with portal venous invasion. *Cancer*. 2006;106:1990-1997.
32. Lam CM, Lo CM, Yuen WK, Liu CL, Fan ST. Prolonged survival in selected patients following surgical resection for pulmonary metastasis from hepatocellular carcinoma. *Br J Surg*. 1998;85:1198-1200.
33. Park JS, Yoon DS, Kim KS, et al. What is the best treatment modality for adrenal metastasis from hepatocellular carcinoma? *J Surg Oncol*. 2007;96:32-36.
34. Une Y, Misawa K, Shimamura T, et al. Treatment of lymph node recurrence in patients with hepatocellular carcinoma. *Surg Today*. 1994;24:606-609.
35. Momoi H, Shimahara Y, Terajima H, et al. Management of adrenal metastasis from hepatocellular carcinoma. *Surg Today*. 2002;32:1035-1041.
36. Poon RT, Fan ST, O'Suilleabhain CB, Wong J. Aggressive management of patients with extrahepatic and intrahepatic recurrences of hepatocellular carcinoma by combined resection and locoregional therapy. *J Am Coll Surg*. 2002;195:311-318.
37. Kaizu T, Karasawa K, Tanaka Y, et al. Radiotherapy for osseous metastases from hepatocellular carcinoma: a

- retrospective study of 57 patients. *Am J Gastroenterol.* 1998;93:2167-2171.
38. Park YJ, Lim do H, Paik SW, et al. Radiation therapy for abdominal lymph node metastasis from hepatocellular carcinoma. *J Gastroenterol.* 2006;41:1099-1106.
39. Chang L, Chen YL, Kao MC. Intracranial metastasis of hepatocellular carcinoma: review of 45 cases. *Surg Neurol.* 2004;62:172-177.
40. Zeng ZC, Tang ZY, Fan J, et al. Radiation therapy for adrenal gland metastases from hepatocellular carcinoma. *Jpn J Clin Oncol.* 2005;35:61-67.
41. Yamakado K, Anai H, Takaki H, et al. Adrenal metastasis from hepatocellular carcinoma: radiofrequency ablation combined with adrenal arterial chemoembolization in 6 patients. *AJR Am J Roentgenol.* 2009;192:W300-W305.
42. Kuehl H, Stattaus J, Forsting M, Antoch G. Transhepatic CT-guided radiofrequency ablation of adrenal metastases from hepatocellular carcinoma. *Cardiovasc Intervent Radiol.* 2008;31:1210-1214.
43. Kashima M, Yamakado K, Takaki H, et al. Radiofrequency ablation for the treatment of bone metastases from hepatocellular carcinoma. *AJR Am J Roentgenol.* 2010;194:536-541.